Power Electronics in Modular Solar Home Systems

Lukas Irazusta Gorostidi

ABOUT THE PICTURE

The cover picture was taken by Dr. Laurens Mackay in the small village Addi Araha which is located in Tigrey, Ethiopia. The capital city of this region is Mekelle and while it is the 5th most populated city in Ethiopia as well as an important academic and economical force, the majority of the households located in the rural areas surrounding the city do not have access to electricity. The picture depicts a number of curious neighbors who are inquisitive about the newly arrived power bank and LED light. These items were brought in the first trip that DC Opportunities made to Ethiopia. After completing this thesis and with a more mature technology, I feel eager to pay a visit in the upcoming months in order to implement a pilot test and reap the rewards of the work put into this project.

POWER ELECTRONICS IN MODULAR

SOLAR HOME SYSTEMS

By

Lukas Irazusta Gorostidi

In partial fulfilment of the requirements for the degree of

Master of Science

Sustainable Energy Technology

at the Delft University of Technology,

to be defended publicly on Friday October 25th , 2019 at 13:30.

Supervisors:	Prof. dr. J.A. Ferreira	TU Delft
	Dr. Laurens Mackay	DC Opportunities R&D
Thesis committee:	Prof. dr. J.A. Ferreira	TU Delft
	Dr. ir. Gautham Ram	TU Delft
	Dr. A.I. Stefanov	TU Delft

This thesis is confidential and cannot be made public until 25th October 2024.

ABSTRACT

Access to electricity is a key actuator in order to tackle poverty in areas of limited resources. While the population without access to electricity has a decreasing tendency, still almost 1 billion people continue to live without this basic amenity.

This thesis has been carried out at the company *DC Opportunities* as part of the rural electrification project. On this field, the main activity focuses on developing cost-effective DC solutions in the form of a solar home system which consists of a total of 4 devices including low-power LED lights, a solar charging station, a high-power rate power bank and a power hub.

The report analyses various existing electrification projects identifying the characteristics of their approaches in order to recognize the shortcomings of market available products and to build a design criterion. Given that the main target application is aimed at rural areas, a modular approach has been the base of the design criterion with the purpose of tailoring the SHS to developing countries with limited resources. The project analyses each step within this modular process together with the power electronics involved in every stage.

The main objective of the project is to perform direct charging between the charging station and the power bank, which consists in feeding power directly from the bus voltage of the charging station into the battery cells with only one active converter. This feature is implemented as a result of the introduction of the power delivery protocol released together with the USB type C connector . This offers a wide variety of possibilities which includes negotiable voltage levels ranging from 5 to 20V.

The first element taking part in the direct charging is the charging station .This thesis addresses the challenge of designing and building a circuit with dynamic adjustment of voltage and current in a cost-effective and reliable manner. By adding a digital to analogue converter and 2 operational amplifiers, it is possible to add this feature to a wide range of standard voltage converters available in the market. The report analyses this circuit in 3 steps: first with circuit theory, secondly by simulation and eventually by including the results obtained in an empirical test implemented in one of the prototypes.

The power delivery protocol is also beneficial for a power-bank application, which is the second element of the direct charging. It is one of the purposes of the thesis to evaluate the performance of direct charging.

Eventually, the report presents the main conclusions derived from the analysis of the aforementioned elements and also covers future lines which include improvements to be implemented within the components of the solar home systems.

PREFACE

This master thesis concludes my studies in Sustainable Energy Technology at TU Delft, but it also marks an end to my academic career which has lasted a total of 6 years. I have been fortunate enough to study in 3 different countries which has provided me enrichment at an educational but also personal level: Mondragon Unibertsitatea in Spain, the Norwegian University of Science and Technology in Norway and the Technical University of Delft in the Netherlands.

This period has been filled with both challenging and rewarding moments. I would like to acknowledge the support system that has strongly contributed to my success which includes my parents, my siblings and the numerous colleagues and friends that I have had the pleasure to encounter throughout this process. I would also like to thank all the university staff that has been part of my academical training and in special to Dr. Laurens Mackay for providing me guidance, teaching me new skills and overall for trusting in me to be part of this adventure.

I now feel strongly motivated to keep developing myself in the field I have been working during my thesis by continuing as an employee in the rural electrification project and by implementing a field test later this year in Ethiopia.

TABLE OF CONTENTS

TABLE OF FIGURES

TABLE OF TABLES

LIST OF ABREVIATIONS

PCB   Printed Circuit Board

BoM   Bill of Materials

SoC   State of Charge

PV   Photovoltaic

BMS   Battery Management System

PAYG   Pay As You Go

MPPT   Maximum Power Point Tracking

SHS   Solar Home System

USB   Universal Serial Bus

DAC   Digital to Analogue Converter

ADC   Analogue to Digital Converter

MCU   Microcontroller Unit

UVLO   Under Voltage Lockout

CC/CV   Constant current/ constant voltage

MOSFET   Metal-oxide-semiconductor Field-effect transistor

PWM   Pulse Width Modulation

DCM   Discontinuous Conduction Mode

IC   Integrated Circuit

1. CHAPTER

INTRODUCTION

This chapter establishes the context in which the thesis takes place by identifying an existing problem to be tackled. In order to achieve so, the tendency and situation of electrification rate is analysed with the purpose of identifying some key elements such as the reasons that prevent a more fruitful proliferation of access to electricity, the disparities between urban and rural areas or the benefits entailed with access to electricity.

In view of this challenge, the objective of the thesis is presented which is revolved around developing prototypes of a SHS and performing direct charging between a solar charging station and a power bank. This is followed by the research questions to be answered throughout the report. Eventually, the outline of the document is presented.

1.1 PROBLEM DEFINITION

Social welfare and quality of life of a specific area are monitored by several indicators including electrification rate. While access to electricity has been proven to be insufficient to tackle poverty, it is a necessary tool. The decreasing tendency of population without access to electricity reached a milestone in 2018 when the total number of people without access fell below 1 billion [1]. However, a large portion of the global population does not yet have access to basic commodities such as lighting. The disparity on how lack of access to electricity is allocated worldwide is represented in Figure 1.

While the countries located in the north hemisphere are fully electrified for the most part, lack of access to electricity is concentrated in Africa, South America and south Asia. In terms of population quantity, the most affected countries are Nigeria, Congo, Ethiopia & India. However, countries like South Sudan, Burundi or Chad hold the most alarming electrification rate which lays below 10%. [2]
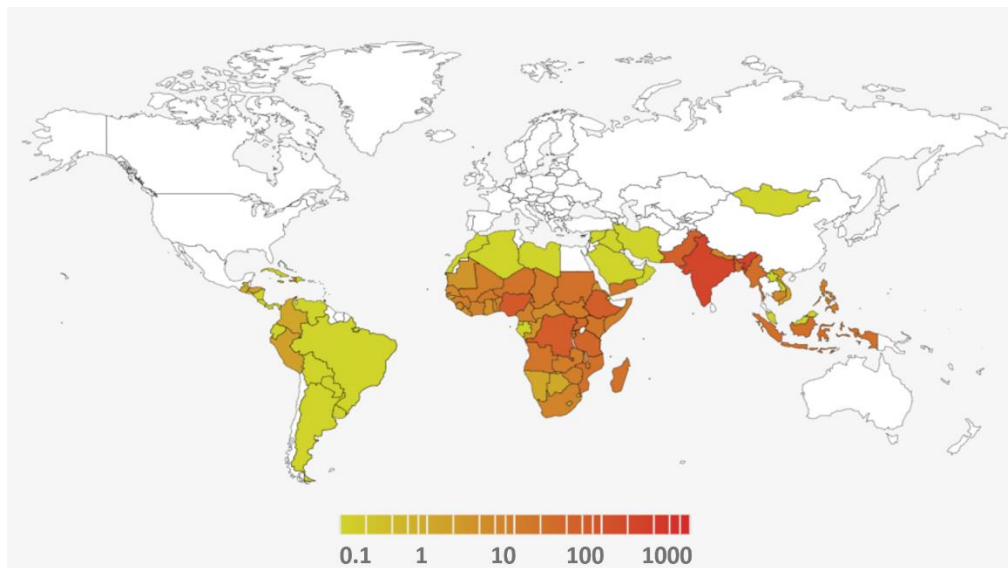
Figure 1: Map of population without access to electricity in 2016, in millions [2]

This part of the population is not homogeneously distributed among urban and rural areas, either. The combination of a low-income population together with the challenges and the socio-economic implications that building an infrastructure in remote areas entails, results in rural areas being especially affected by lack of access to electricity. Following similar patterns of those in Figure 1, the percentage of rural population with access to electricity lays on 48.4% for South Asia and only 11.9% for Sub-Saharan Africa [3].

It is important to bear in mind that the challenges associated with each country are accentuated in different areas. An insightful example would the juxtaposition between India and Ethiopia. India tops the list of countries with most inhabitants lacking access to electricity and given its high population density, building a grid infrastructure to interconnect households is a relatively feasible solution in some areas of the country. Whereas in the case of Ethiopia, the low population density together with its mountainous geography result in stand-alone solutions being the only possible alternative to bring electricity.

The idea that electrification of rural areas is a vital driving force for the development of rural areas has led to governments of developing countries giving priority to investing in projects of this nature. Furthermore, rural electrification is strongly linked to sustainability and climate change. As a result, many organizations have supported projects that research on the integration of decentralized renewable sources and rural electrification is a prevalent application. These include Global Environment Facility (GEF), the Prototype Carbon Fund (PCF) or Joint Implementation (JI) to name a few [4]. The result of this is plotted in Figure 2 which displays the access to electricity rate throughout the last decades.
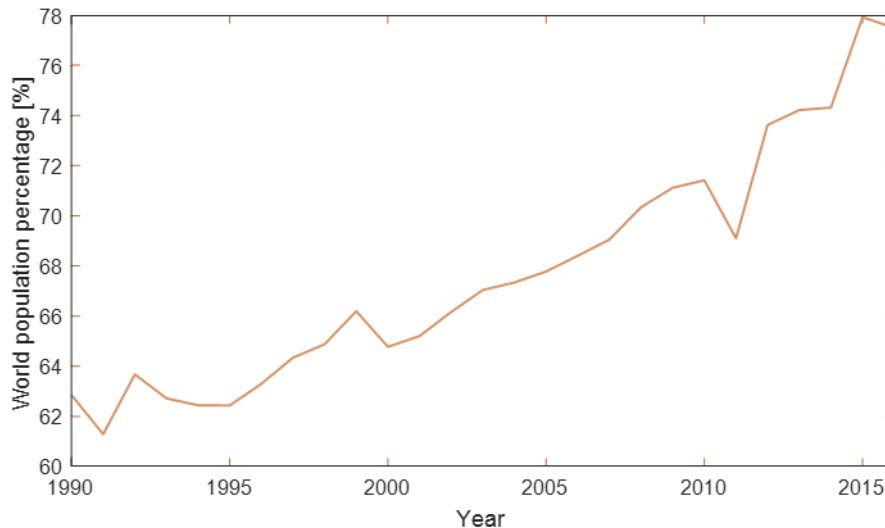
Figure 2: Graph showing access to electricity rate from 1990 to 2016 [2]

However, this growth has not always followed the pace that was intended, this is specifically noticeable in the year 2011 for instance. The World Bank has identified the reasons behind these setbacks based on 120 projects it has supported since 1995 and has taken a new approach [3]:

- Focusing mainly on cost recovery criteria has been adjusted in order to meet the needs of areas affected by poverty. The new criterion is based on operating and maintenance costs, if the local income can cover these, subsidies are justified.
- Rural electrification projects must be complemented with educational initiatives that will encourage the final user to put energy into productive uses.
- An independent and effective agency is required. The task of this institution is ensuring that the plans for electrification can be delivered.

Another relevant point is that there is a significant difference between the electrification process of the industrialised countries in 1900 and the rural electrification of developing countries in Figure 2. While share the same goal, the first case involved developed economies with a strong infrastructure that were in the position to invest in electrification. The fact that these are happening almost a century apart sets a different context: new technologies are available nowadays at an affordable price, as a result the presence of decentralised PV for example is prevalent in the electrification of developing countries.

As aforementioned, access to electricity is not a solution to tackle poverty but rather a tool. Lack of electricity prevents rural areas from socio-economic development. Providing access to electricity implies increasing living standards of locals by improving several areas [5]:

- Safety: providing illumination in public spaces reduces the criminality rate.
- Health: the dominant light-source in most rural areas are kerosene lamps, which have been proven to be detrimental for the health.
- Environmental: If kerosene lamps were to be substituted by PV in mass-scale, this would even have an impact on black carbon emissions globally.
- Communication: together with lighting, the end-user service with highest demand is charging mobile phones. Mobile phones prevent the isolation of rural areas and they are also a dominantly common tool to make payments.
- Economical: productivity in the household and in local businesses is increased by allowing working hours after sunset. This can alleviate poverty together with not having to buy kerosene. SHS also create small businesses such as phone charging kiosks.

1.2 OBJECTIVES

The main goal of the thesis is designing and building prototypes of a SHS tailored for rural areas in developing countries.

The purpose of the project is to develop a solution to provide electricity within the context of rural areas in developing countries. The task within this project is to design and to build various prototypes as part of a Solar Home System. Given that the design is tailored to areas with limited resources, modularity is one of the main components of the design criterion together with direct charging. By utilizing USB type C connectors, battery cells can be charged via direct charging. Hence, the hardware is designed with this functionality in mind. As a result, the objective is to design and to build the elements that belong to the first stages of electrification: LED lights, solar charging station, high power-rate power-bank and power hub.

1.3 RESEARCH QUESTIONS

In the path to accomplishing the aforementioned objectives, there are some research questions that are addressed throughout the report. In the context of SHS design, 3 questions will be tackled:

1.3.1 HOW TO ADD DYNAMIC ADJUSTMENT OF VOLTAGE AND CURRENT FEATURE TO A STANDARD CONVERTER?

In order to be able to perform direct charging, the components within the SHS must be equipped with the hardware that allows this functionality. This is especially important for the solar charging station which requires dynamic adjustment of voltage and current. By implementing this feature, a wide range of loads can be connected while optimizing battery charging, given that the output voltage can be configured so that power can directly be fed into the cells reducing the number of active converters.

1.3.2 HOW TO DESIGN A HIGH-POWER RATE POWER BANK WITH DIRECT/FAST CHARGING?

The key element to allow users to bring electricity within their household are portable energy storage systems, for this project a power-bank. In an attempt to optimize and tailor this components for rural electrification, offering the option of fast charging is an important added value. For users who cannot charge the power-banks at home it is an inconvenience to wait for long periods while the battery charges at the kiosk. As a result, the second research question to be addressed is how to develop a high power-rate power-bank with the option of charging and discharging at high power-rates. A factor that is necessary to take into account is the cost, developing an affordable element increments the scale of insertion of the power-bank into users' everyday life.

1.3.3 WHAT ARE THE BENEFITS OF DIRECT BATTERY CHARGING WITH TYPE C CONNECTION?

As a result of the introduction of USB-C connector and the power delivery protocol, USB connections can reach up to 20V. This offers a wide range of possibilities, direct charging being of them. Power can be fed into the battery cells directly without conversion losses. This results in a higher efficiency as well as a lower charging time. This is the focus of the last research question, to analyse this tendency by carrying out tests with the prototypes.

1.4 THESIS OUTLINE

The content collected throughout the thesis period is recapitulated in this report which consists of a total of 7 chapters including the introductory one. In an attempt to establish the context where the thesis has been carried out, Chapter 1 Introduction presents the problem to be tackled by analysing the current state of rural electrification worldwide. The objectives to be achieved in the thesis are defined as well as the research questions to be answered throughout the process.

Chapter 2 Literature review includes a literature study by making research on the solutions that have been used in the past to bring light or electricity to rural areas. However, the focus of this chapter is on emerging solutions such as SHS which have long-term electrification as a goal. Various existing projects with different approaches are analysed in order to identify the limitations and advantages of each strategy for different applications.

This research is the base to form a design criterion as explained in Chapter 3 Trajectory to electrification . One of the main pillars of the SHS designed for this project is its modular nature. Based on the premise that some rural areas have little or no access to electricity, the introduction of electricity must be performed at a gradual pace. This segment goes through all the steps in order to achieve a reliable long-term solution, focusing on the hardware utilized in each step which has been designed tailored for this application.

One of the main added values within the SHS and hence, one of the key elements to be analysed is charging a power-bank with direct charging. In the SHS, the power-banks are charged via a solar charging station. Taking advantage of the USB type C power delivery protocol, USB connectors can have voltages up to 20V which enables regulating the outputs of the station to the voltage of the battery cells without the need of adding a converter to boost the voltage. Chapter 4 Dynamic adjustment of voltage and current presents the design of the solar charging station and focuses on the circuit that has been implemented in each of the ports to achieve dynamic adjustment of voltage and current.

The second component taking part in direct charging is the power-bank itself, this has also been designed for the project. The design of this element is discussed in Chapter 5 High power-rate power-bank. First, the requirements of the power-bank are listed in order to build a design criterion, followed by the design of the power bank is presented by including the software design as well as a physical prototype identifying where the main components are located. This segment also includes a second revision of the power ban where the updated criterion is discussed, and a new prototype is presented.

Once both the solar charging station and the high-power rate power-bank have been analysed, Chapter 6 Battery charging is focused on the results obtained after performing tests with the prototypes. The segment presents results from direct charging and making a comparison with a regular USB charging cycle. The switching patterns of the Buck and Boost converters are also discussed.

Eventually, the final chapter of the report, Chapter 7 Conclusions, summarizes the conclusions drawn throughout the thesis. The research questions defined in chapter 1 are discussed in this segment and a number of future lines are also included, shedding light on the improvements to be implemented within the SHS to achieve its full potential.

2. CHAPTER

LITERATURE REVIEW

The first segment of this chapter presents the technologies that have been utilized in the past to provide lighting to rural areas, as well as more recent solutions which have electrification as a goal. The purpose of this analysis is to identify the drawbacks and benefits of each solution to have a better understanding of the tendency within the rural electrification field. The chapter also includes a comparison of the most relevant characteristics such as aspects involving cost, scalability or availability.

The main focus of the segment are solar home systems. While there are numerous ongoing projects involving rural electrification, there are many possible approaches in terms of policy and technologies. 3 of these projects are analysed in detail in order to recognise the benefits and limitations of different approaches based on their applications. This analysis is necessary to build a criterion when designing a solar home system.

2.1 EXISTING SOLUTIONS FOR LIGHTING & ELECTRIFICATION

This section analyses the existing solutions to bring commodities to rural areas, which are divided into 2 categories based on their nature: conventional solutions which are limited to lighting and emerging technologies that have full electrification as a goal. This segment also includes a comparison between the technologies identifying the limitations of each.

2.1.1 CONVENTIONAL SOLUTIONS

For many years, kerosene has been one of the leading resources utilized for lighting (Figure 3 A depicts a kerosene-based lamp) in developing countries. While it is often advocated as a clean substitute to solid fuels like wood or coal, the combustion of kerosene implies the exposure to exhaust gases that imply health risks linked to lung infection, asthma, cancer and susceptibility to infectious diseases such as tuberculosis. [6]

It has already been discussed in section 0 that a disparity is notorious between rural and urban areas as far as electrification rate is concerned. One factor that contributes to accentuating this contrast is the price difference of kerosene. A study carried out in Senegal, Mali, Ghana, Tanzania and Kenya suggests that the average price per litre of kerosene in rural areas is 35% more expensive than in urban areas [7].

The reason behind lays in the facts that rural villagers buy kerosene in smaller volumes which results in a high per unit price, as well as the added cost of transporting to remote areas. One of the consequences is the resulting higher payback period for non-urban environments. As a result, rural areas find more economic benefit in utilizing solar photovoltaic technologies.

Another leading energy source for this applications are disposable batteries. While batteries do not release exhaust gases, the mass use of disposable batteries can be significantly harmful for the environment as improper disposal of used batteries can pollute soil and groundwater. [5]

Figure 3: A) Kerosene lamp B) Solar lantern

In consideration of the environmental damage caused by the aforementioned solutions, solar lanterns became popular as substitutes for lighting solutions. Solar lanterns consist of a luminaire based either on CFL or LED within a plastic or metal enclosure and a rechargeable battery and necessary electronics. An example of this is shown in Figure 3 B.

The battery is charged via a PV module which can be either external or integrated within the lantern. The advantages of solar lanterns include versatility and portability while tackling the environmental damage challenge. However, the potential of this technology is limited to lighting and it does not provide a solution for complete electrification of households. [8]

2.1.2 EMERGING SOLUTIONS

On the context of rural electrification on the topic of cost-effective solutions, the most prominent solution that has emerged in the past decades are Solar Home Systems (SHS). SHS consist of stand-alone configurations based on a photovoltaic source, a storage battery, a controller for the battery and end-user appliances. These systems offer an alternative to remote areas where building an electrical infrastructure is economically not viable.

Photovoltaic systems gained global market share after the energy crisis of the 1970's [9] driven by 2 main reasons; firstly, the shortage of fossil fuels resulted in policies gaining interest in renewable sources, especially photovoltaic. The ongoing research on PV materials and configurations results in PV becoming the most economically competitive source. Figure 4 displays the evolution of the price of photovoltaic power per peak-watt in American Dollars throughout the last 4 decades. It is no surprise that having reached a historic price of 0.30$/Wp PV is the source for SHS. Secondly, the concern for the environment strengthened, global warming becoming the base for many policies and regulations.
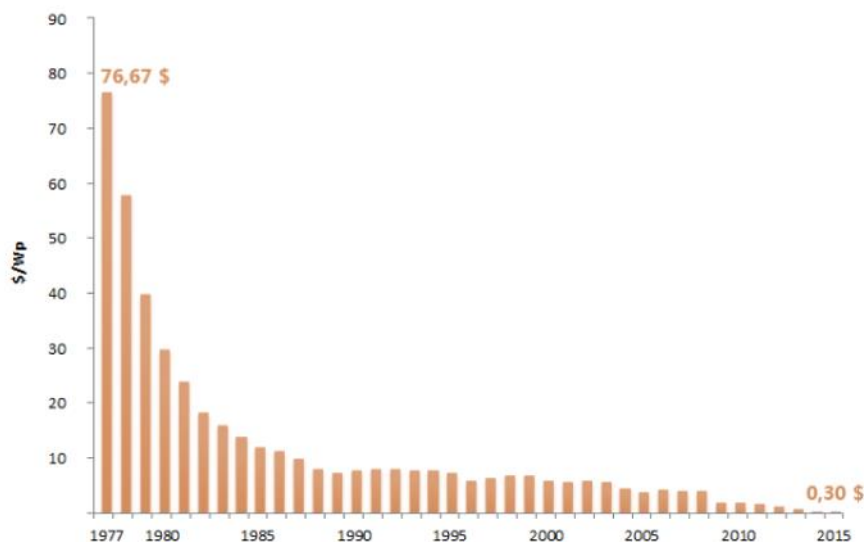
Figure 4: Bar-graph with evolution of PV price from 1977 to 2015 [10]

2.1.3 COMPARISON OF SOLUTIONS

After analyzing each of the technologies individually, Table 1 summarizes their characteristics in order to make a comparison and to identify the benefits and drawbacks. As far as cost is concerned, even though the kerosene lamp leads the top position with the least initial costs, its variable costs are high compared to the other 2 options given that they have no variable costs.

This leads to the conclusion that in the long run the 2 renewable sources would break even and result economically more attractive than the kerosene lamps. However, it is also important to take into account that the maintenance and replacement cost of these technologies is considerably higher than that of kerosene lamp as a result of the scarce resources and availability of parts and technical services in rural areas.

Furthermore, from a sustainability and safety point of view it can be concluded that kerosene lamps are not a viable solution given the health and hazard risks entailed with it. Since solar lanterns are based on a renewable source and no combustion is involved, they achieve to tackle this problem. However, their application is limited to lighting and proves to be insufficient to fully electrify a household or community.

Based on this comparison, solar home systems present the most promising features to tackle lack of access to electricity in rural areas and hence provide a tool to combat poverty. Nevertheless, there are some key challenges attached to it such as the high upfront cost and the lack of availability of products to be able to perform reparations and maintenance is a cost-effective manner.

Table 1: Comparison of existing solutions for rural electrification [8]

Characteristics	Kerosene lamp	Solar lantern	Solar Home System
Capital cost	Low	Medium	High
Fuel cost	High	Null	Null
Replacement cost	Low	High	Very high
Availability and reparability	Very good	Poor	Very poor
Lumen output	Low	High	Very high
Scalability	Limited	Limited	Wide range
Electrification	Limited to lighting	Limited to lighting	Full electrification
Safety	Fire and health hazards	Safe	Safe

2.2 SOLAR HOME SYSTEMS

Stand-alone Solar Home Systems have gained popularity in sparsely populated areas in the past decade, leading to the development of numerous projects that seek an effective solution for electrification in low-income areas. The purpose of this chapter is to make an analysis on existing projects in order to set a context on currently used technologies and policies. By identifying the shortcomings of market available products, it is possible to form a criterion to develop a system tailored for rural electrification.

2.2.1 EXISTING PROJECTS

Africa is the continent that hosts the majority of electrification projects. While they all share the same goal, the path to accomplish a successful electrification is different for each case in terms of technology and policies. As far as payment methods are concerned, the prominent option in rural areas is the Pay-As-You-Go (PAYG). This concept is not pioneering given that it has been widely used in the mobile industry, however its application in rural electrification is innovative. PAYG is based on pre-paid deals that prevent the customers from having to face the high upfront cost of SHS. 2 approaches can be distinguished within the PAYG payment method [11]:

- Rent-to-own: customers pay an initial price when purchasing the SHS and afterwards, a monthly/weekly/daily fee is applied. If customers fail to pay this fee the system is automatically blocked. After a certain amount of payments, the customers become owners of the system and this is unlocked for an unlimited time.
- Service: some companies do not sell the system itself but rather the energy produced by it. In this type of businesses, the company also ensures proper operation of the device by providing reparation and maintenance services. In both cases customers have a periodical payment that in case they fail to pay, they lose access to the system. However, in this option customers do not become owners of the SHS.

Table 2 summarizes the characteristics of 3 ongoing projects in Africa. These have been chosen based on the fact that each case provides a new characteristic on their approach.

Table 2: Characteristics of existing rural electrification projects in Africa

Company	Countries	Payment method	Solar Home System
FRES	Mali, South Africa, Burkina Faso, Uganda & Guinea Bissau	Service	Focused on creating small local companies. Different service levels.
Angaza Design	Kenya, Tanzania, Uganda, Zambia	Rent-to-own	PicoPV LED lamp, 3W solar panel and a hub with phone charger and 3Ah battery.
Azuri Technologies	Ghana, Kenya, Malawi, Rwanda, Tanzania, Uganda etc.	Rent-to-own	Solar panel connected to a central box which includes connectors and the control. It offers different service levels.

The Foundation Rural Energy (FRES) is a Dutch institution that focuses its activity in founding local small businesses to provide electricity to households from solar energy. Given that FRES is present in a total of 5 countries in Africa, it is an umbrella foundation for various small companies that offer different products dependent on the resources, environment and demand of each region. FRES offers different service levels ranging from 2 lamps or 1 socket outlet to 3 lamps and 1 socket outlet. As far as payment method is concerned, FRES bases its activity on Service PAYG where users pay for the energy consumed. Under this premise, the companies also guarantee proper operation the system providing maintenance and repairing services.

However, the fact that the users do not feel ownership of the system can have an impact on the usage habits they have and the treatment they give to it. It is plausible to expect a less cautious treatment of the SHS. [11]

This matter is tackled by Angaza Design which utilizes the rent-to-own PAYG as payment method, while users are committed to a regular payment, eventually they do become owners of the system. Angaza Design focuses on picoPV systems which consists of a 3W PV panel, a LED lamp and a mobile-phone charger. This charger also features a 3000mAh battery.

Nevertheless, there are some drawbacks to this system: users must have access to network in order to make the payment as well as to activate the credit. This can entail challenges given that availability of network cannot be assumed to be everywhere. Furthermore, Anganza Design does not provide scalability of their product and given that they work with picoPV, the applications are limited. As a result, it is a solution for lighting and phone charging to a certain extent but prevents the possibility to power bigger household loads such as radio or television.

Azuri Technologies is one of the companies with most presence in Africa, it has projects in Ghana, Kenya, Malawi, Rwanda, South Africa, South Sudan, Tanzania and Uganda. It is one of the pioneer companies offering PAYG payment. Unlike, Anganza Design, Azuri Technologies offers a wide range of products that meet the demand of each customer. Their products range from a 3W "Light" service level which can power a mobile phone and 2 LED lamps to a "Work" service level of 80W which adds capability to power a radio TV, sewing machine etc.

Azuri technologies provides a solution to the aforementioned matters, users feel an ownership of the system and the product offers scalability according to the needs of each user. However, it is estimated that it takes 18 months on average to pay off the system which can be long.

Customers of SHS often live in rural areas with low-income population whose main activity is farming. As a result, farmers rely on crops which prevents them from having a stable income. Hence, they cannot take the commitment to pay a monthly fee and if they do, and fail to pay the fee, the system will be blocked. It is also important to bear in mind that these agreements entail a high risk for both the customer and the supplier. This risk results in high interest rates which are added to the fees. As a result, the customer eventually pays a total amount that is equal to the double or triple of the original SHS price. [12]

3. CHAPTER

TRAJECTORY TO ELECTRIFICATION

The final goal of the rural electrification project is to provide a reliable low-voltage grid within rural areas. However, different approaches can be taken to achieve this which depend on factors such as environment or application. The target of this project are remote rural areas or located in mountainous environments that prevent the possibility of connecting to the main grid. The solution for these cases are island-mode micro-grids.

However, the path to a microgrid entails various prior steps. Given that the inhabitants within these rural areas do not have access to electricity locally, the introduction of this amenity must be gradual. By implementing a modular system, users can decide how much capacity they want to purchase and at what pace.

This chapter is divided into 3 parts which cover different aspects within the path to electrification. The first segment presents the criterion for the design of the SHS, this has been formed by analysing existing projects and analysing the necessary key elements for the intended application. The second segment includes the steps from no access at all to a low-voltage micro-grid. The steps are complemented with visual representations of the state of the SHS in each steps as well as a description of the commodities the user has. The final segment focuses on the power-electronics involved throughout the process. The main features of all the hardware components are discussed.

3.1 CRITERION FOR THE DESIGN OF A SHS

In view of the characteristics and shortcomings of existing technologies, DC Opportunities seeks to develop a SHS to provide an effective solution for lack of access to electricity in rural areas of developing countries. Given that the purpose of this thesis is developing prototypes for a SHS, it is important to specify the characteristics that the system should have.

3.1.1 FULL ELECTRIFICATION

Access to electricity is a key-tool to tackle poverty in rural areas, but in order to accomplish a successful electrification the goal of the project needs to be seeking a long-term solution to provide a reliable community-level grid. As a result, the system should not be limited to only lighting, but it should also provide the option to connect higher loads and eventually interconnect the households to trade energy.

3.1.2 SCALABILITY

Under the premise that access to electricity is inexistent, the process of electricity introduction should happen in a progressive manner. Consequently, there should be a range of products in offer that responds to different needs of energy levels. Customers should be able to purchase an initial device as a first step to introduce electricity in their routine. Subsequently, when a need for higher capacity or comfort exists, users can acquire a second device in an attempt to reach full electrification.

3.1.3 AFFORDABILITY

The majority of customers cannot afford to pay the totality of the SHS upfront costs. While PAYG is the prominent option for these applications, it involves a risk for both supplier and customer resulting in a long-term commitment of monthly fees and resulting a significant increase from the original price for the user.

This risk together with the volatility of incomes of locals, prevents a faster diffusion of solar stand-alone systems. The solution to avoid periodical payments relies on modularity. Since the cost of the entire SHS is too high to be purchased upfront, parts of the system can be acquired gradually enabling a progressive introduction of electricity within the households. Parts of the SHS are sold separately providing several levels of capacity reducing the price significantly.

3.1.4 WIDE RANGE OF LOADS

One of the main limitations of existing SHS is that they only offer the possibility to connect low-power loads. This not only is limited by the capacity of the source but also by the output USB connector. Conventional USB connectors can charge with a maximum of 1.5A according to the Battery Charging Specification 1.2. [13]

Since the introduction of the type C USB connector, the consumer electronics is shifting towards providing higher power via USB connection. This connector supports power delivery protocol which allows output voltages up to 20V and currents up to 5A. The maximum output power of this connector is 100W which is 40 times greater than conventional USB. [14]

Besides higher power, USB-C also provides other features such as bidirectional power flow and a reversible connector. These features are key tools in order to achieve direct battery charging and it also allows connecting higher power loads such as radio, television etc.

3.1.5 EFFICIENCY

The possibility to achieve voltage up to 20V with power delivery, offers a range of features that can be added to the SHS. As far as storage mechanisms and portable power-banks are concerned, battery cells are conventionally connected in parallel given that the bus voltage needs to be supported by USB. USB-C provides the option of connecting cells in series reducing the current throughout the bus voltage and, hence increasing efficiency.

Furthermore, by negotiating the voltage level of the connector, power can be directly fed into the bus voltage of the power bank and hence into the battery cells with no conversion losses. This is denominated as direct charging.

3.2 STAGES OF ELECTRICITY INTRODUCTION

The rural electrification project carried out within DC Opportunities focuses on offering a variety of components that the SHS consists of. Each of these components belongs to a different stage within the electrification process. This chapter analyses each of this phases and the services provided to users:

3.2.1 STAGE 1: CHARGING MOBILE PHONES AT KIOSK

At the first step on the electrification process, a solar charging station is placed at a local kiosk. The person who runs the shop purchases the PV panel and the charging station to provide a new service as depicted in Figure 5. Users can charge their mobile phones by connecting them to one of the several ports of the device and the price is dependent on charging time and capacity.
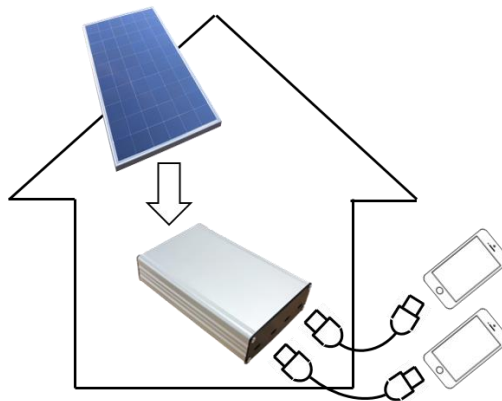
Figure 5: Stage 1: Charging mobile phones at kiosk

3.2.2 STAGE 2: TAKING POWER HOME WITH A POWER-BANK

For the second stage, users that want to take electricity to their households can purchase a power bank that is charged in the solar charging station as shown in Figure 6. By having access to electricity in the house, users can supply basic loads such as lighting or charge the mobile phones. This improvement will allow users have to visit the kiosk with less frequency.
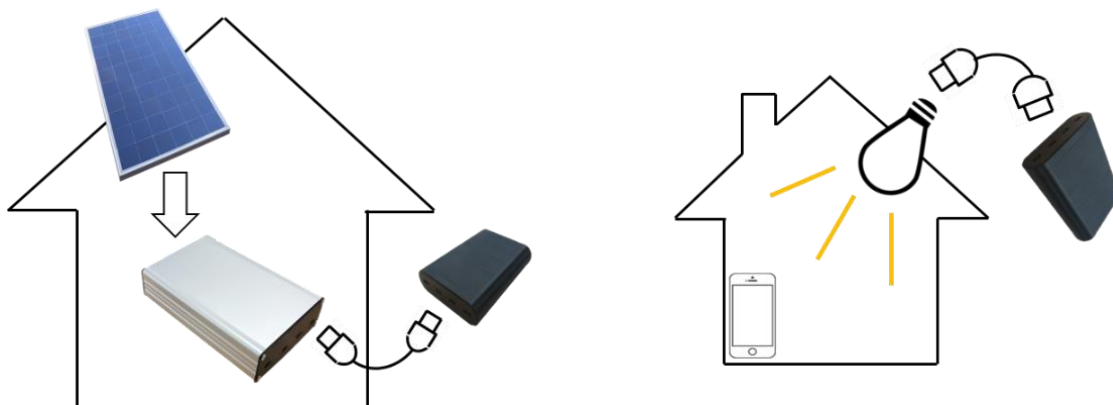
Figure 6: Stage 2: Taking power home with a power-bank

3.2.3 STAGE 3: INSTALLING PV PANELS ON THE HOUSE

The frequency with which users need to go to the local kiosk to charge the power bank will depend on their consumption habits: number of loads and hours of usage. When this consumption is high enough users have the possibility to have local generation and hence, avoid having to visit the kiosk regularly as well as stop paying for charging the power bank.

As represented in Figure 7 solar panels are installed on the rooftop of the household and with a MPPT interface, this can be connected to an input of the power bank. Lights and mobile phones can be connected to the rest of the ports.
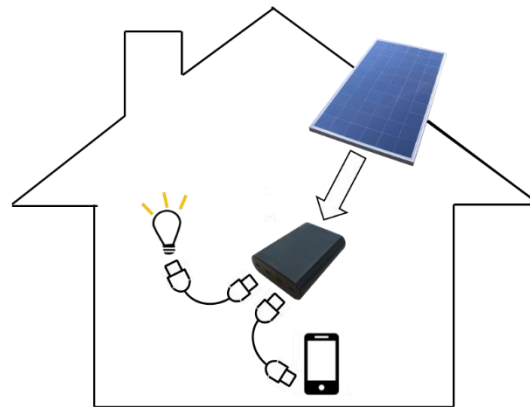
Figure 7: Stage 3: Installing PV panels on the house

3.2.4 STAGE 4: HIGH-POWER STATIONARY LOADS

Given that at stage 3, electricity is already part of the household, users might develop needs to connect a higher number of loads, connect them longer and also power higher power loads. This can be achieved by purchasing a power hub that will serve as a central device of the SHS.

The power hub consists of several high-power outputs to a large number of loads. The hub also counts with touch key sensors to provide comfort to the user when switching the loads, given that at this point loads will be stationary. At this stage customers can power loads such as a television or a radio as shown in Figure 8.
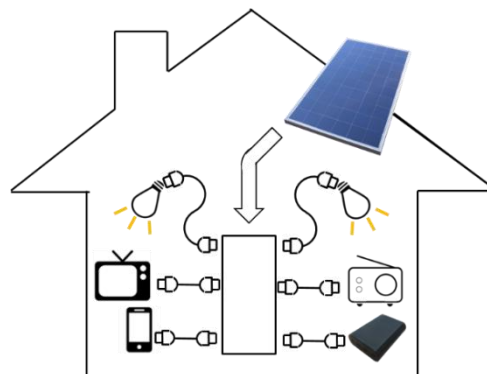
Figure 8: Stage: High-power stationary loads

3.2.5 STAGE 5: LOW VOLTAGE MICROGRID

The finals stage of the rural electrification process refers to a long-term scenario where electricity is part of various households within the community. At this stage, the voltage of the power hub is boosted to a low voltage grid of $\pm 350V$. The houses are interconnected via this grid as shown in Figure 9. [15]

The households can be at different stages of the electrification process, while some of them might have local generation, other houses could just be connected to consume power. At this final stage, from a financial point of view, it is more cost-effective to have community PV generation and storage.
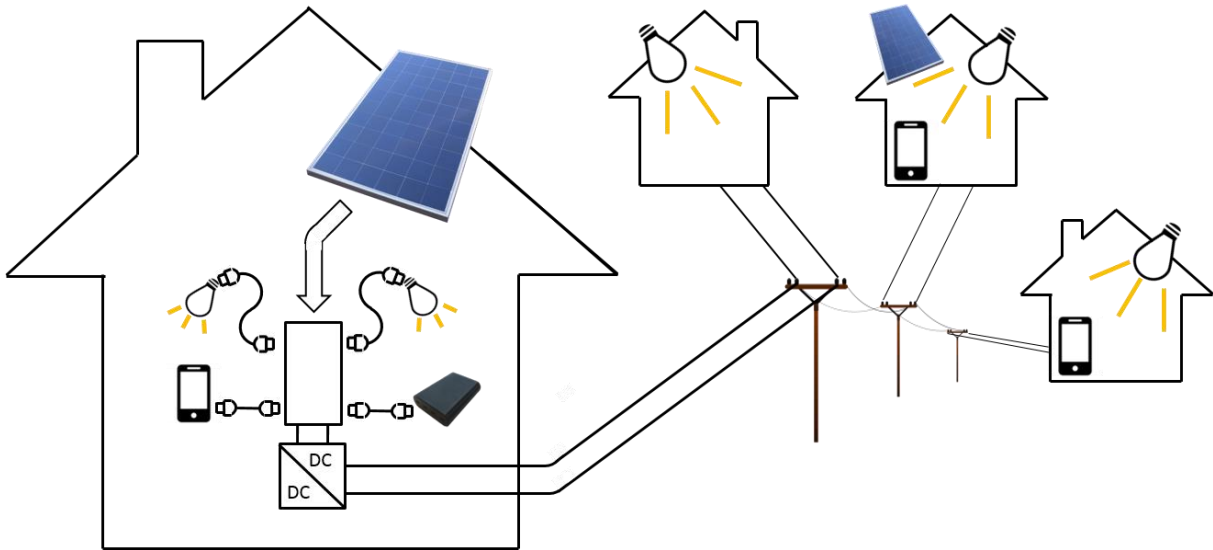
Figure 9: Stage 5: Low-voltage microgrid

3.3 POWER ELECTRONICS IN THE SHS

One of the key points of the project is to develop all the hardware so that all the devices that the SHS consists of meet the aforementioned requirements as well as being compatible with a wide range of other products. This section includes the 4 elements that have been developed as part of the thesis.

3.3.1 LED LIGHT

Lighting is the basic load of a household, the component shown in Figure 10 consists of a USB type C connector that powers 3 homogeneously distributed LED lights. Based on the criterion of efficiency, the total consumption of the lights is 2W while providing 312 lumens [16]. A circular casing has been designed and 3D printed to optimize light diffusion in all angles.
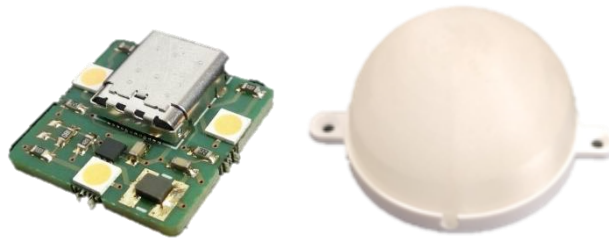
Figure 10: PCB of a LED prototype & its 3D printed case

3.3.2 SOLAR CHARGING STATION

As explained in 3.2.1, the solar charging station shown in Figure 11 is the central element of energy source. Regarding the inputs/outputs of the device, it consists of a PV input that is directly connected to a MPPT converter, a bidirectional Buck/Boost converter for external battery connection and 4 USB-C output ports that can provide up to 60W each. Given that each port has its own converter the maximum power that the station can provide is 240W.

The charging station also features a Raspberry PI [17] with Bluetooth communication. Given that various users will be connected to the station, the wireless communication will allow to identify who the connected device belongs to and also establish the price based on the time connected. This device will be further explained in detail in 4.1.

Figure 11: PCB of a solar charging station prototype and its case

3.3.3 POWER BANK

The high-power rate power-bank is introduced in 3.2.2 as a solution to bring electricity to the household. Unlike the majority of market-available power-banks, the battery cells in the design depicted in Figure 12 are connected in series as opposed to parallel. This enables higher bus voltage and therefore decreases the current together with the thermal losses.

The power bank features a total of 4 USB-C ports with one appointed as the high-power port. This bidirectional port can perform direct charging from the solar charging station feeding power directly into the battery cells while performing current control. It also offers the possibility to connect sources that do not feature direct charging as it is equipped with a boost converter that also feeds into the bus voltage. Hence, this port can also provide high-power on the output while the rest of the ports are connected to smaller loads of 5V.

Following the scalability criterion that the design is based on, the power-bank can be connected to a 4-cell configuration battery bank as well as to a 8 cell configuration, in order to provide higher capacities.

Figure 12: PCB of a power-bank prototype and its 3D printed case

3.3.4 POWER HUB

The final device designed as part of the thesis is a power hub depicted Figure 13. This element can be used to distribute power flows into various output ports of 60W each. It consists of a total of 8 ports:

- Port 0 allows bidirectional power flow with only direct charging as input and voltage control as output. The power bank can be connected in this port through direct charging.
- Port 1 is allocated as a source; this port is connected to a boost converter. A PV panel can be connected here through a MPPT interface, as well as other sources with voltage ranging from 6 to 60V.
- Ports 2 to 7 ports are exclusively output ports where loads are connected.

Even though each port has adjustable voltage, the maximum power that can be provided is 200W by withdrawing 100W from ports 0 and 1.The power hub also features other functionalities such as touch key sensors. Given that some of the loads will be stationary at this point, a capacitive touch key sensor is located in each port, allowing users to switch on or off the loads without the need of connecting or disconnecting the cable. It also could serve to control some lights such as dimming lights.
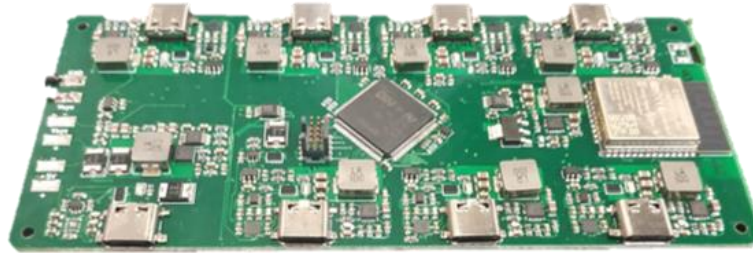
Figure 13: PCB of a power hub prototype

4. CHAPTER

DYNAMIC ADJUSTMENT OF VOLTAGE & CURRENT

The USB-C power delivery protocol offers a variety of features including a wide range of voltage and current levels. Following this innovation, the applications of USB have also evolved in a direction of higher power devices. To complete this cycle, one last area is to be adjusted: converters. While USB output converters have traditionally had a constant output, USB-C allows a circuit infrastructure that will enable taking full advantage of USB-C.

This is specifically interesting for the topic of rural electrification. Being able to adjust the output voltage and current of the converter dynamically offers a variety of applications: connecting a wide range of loads up to 100W with the required voltage level for each case as well as performing direct charging of a battery.

The purpose of this chapter is to analyse how to implement this feature within a converter with 2 main objective functions: reliability and cost-effectiveness. This is presented in a gradual manner: initially constant output voltage followed by dynamic voltage adjustment by adding 2 operational amplifiers. Eventually, this section also analysis current limitation in the output. The selection criterion of each component is explained throughout the chapter.

For this project, this dynamic voltage and current adjustment is implemented in the solar charging station. The operation and functionalities of this device are discussed in the chapter as well as an overall look on the design & manufacturing process.

Once the circuit is designed for the solar charging station application, this is simulated in TINA-TI. After building various charging stations, similar tests are performed to validate the proper operation of the device. The empirical, theoretical and simulation results are compared, and the behaviour of the voltage and current adjustment is discussed.

4.1 SOLAR CHARGING STATION

The general scheme of the solar charging station is illustrated in Figure 14 where the most relevant components of the device are represented. The charging station has a total of 6 power input/outputs: 4 unidirectional USB-C output ports, a Maximum Power Point Tracking input where PV panels are connected and a bidirectional converter connection where batteries are placed. The station also consists of a microcontroller that runs the desired operation within the components.
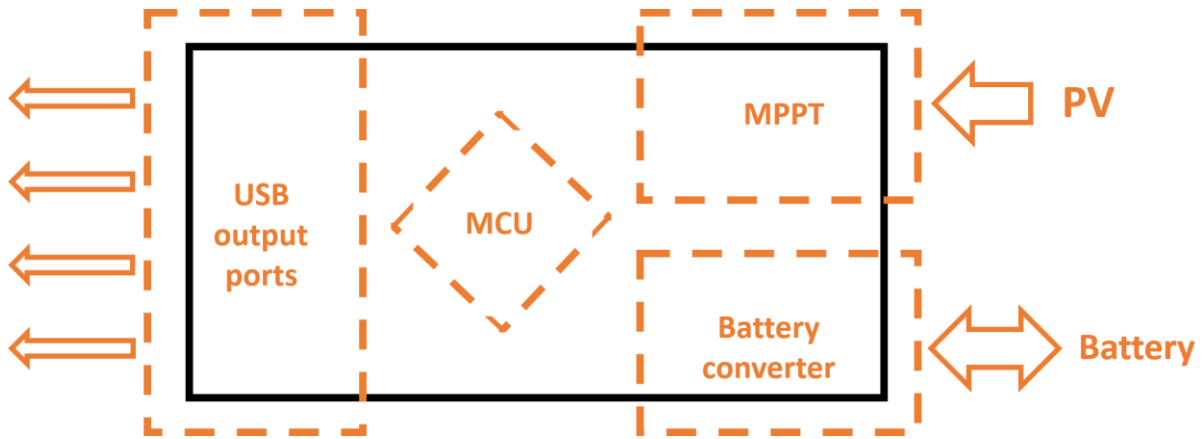
Figure 14: Scheme of the charging station

The basic operation of the solar charging station is the following: energy is supplied by the photovoltaic source through the MPPT interface and this is fed into the 24V bus voltage. This bus voltage is the input of the USB-C port converters that can be connected to various loads. If no loads are connected or the demand is smaller than the PV generation, this extra energy is stored within the batteries. Similarly, when the PV source is insufficient to cover the load at a given time, the battery will support supplying the demand by discharging.

The dynamic voltage and current adjustment is installed within these output ports. By doing so, a wide variety of loads can be connected, and a current limitation can be performed according to the number of loads connected at each given time or according to the type of load. This feature plays a vital role for direct charging of batteries.

The charging station has been first developed on the software for electronic design Eagle. This process is divided into 2 parts: the schematic and board layout represented in Figure 15.
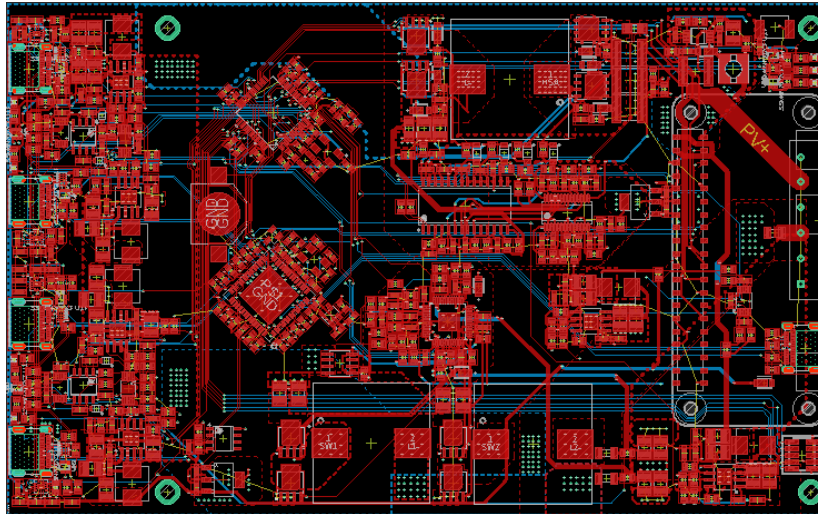
Figure 15: Layout of solar charging station

Once the design is finished on Eagle, the next step was building the physical board with the components selected in the design. The result is in Figure 16 which distinguishes 5 of the main sections:

1. USB-C output ports
2. MCU
3. PV input and MPPT interface
4. Bidirectional battery converter
5. Vertical connector for Raspberry PI. This component enables Bluetooth communication.
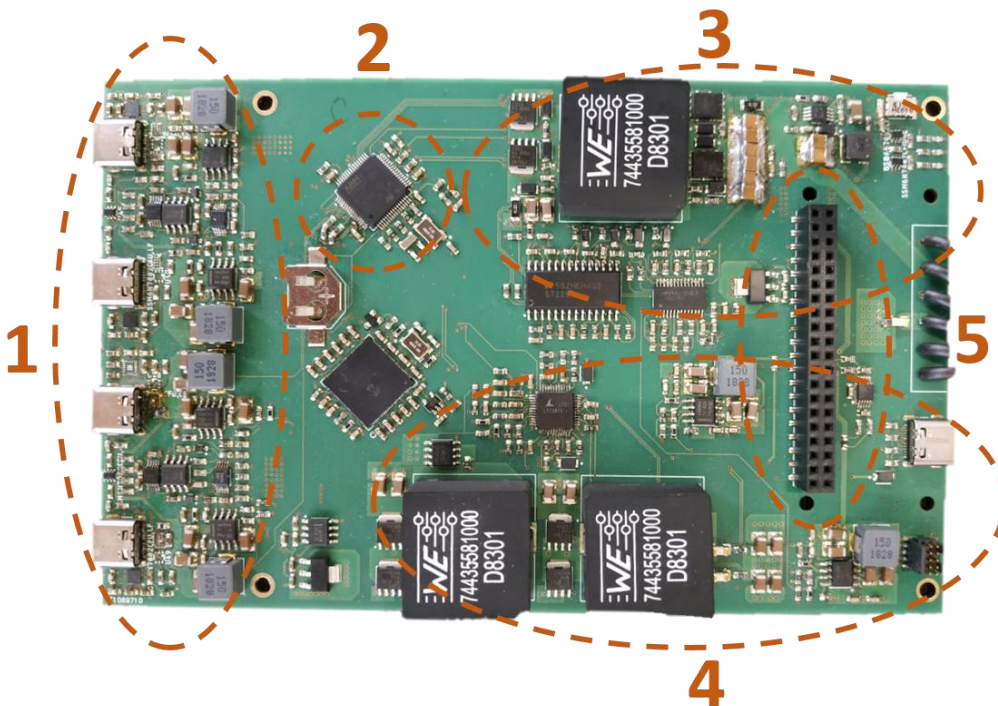
Figure 16: Prototype of solar charging station with highlighted components

4.2 VOLTAGE ADJUSTMENT

This section analyses 2 circuits to achieve output voltage control. Firstly, the configuration for constant voltage is presented. Second, a digital-to-analogue converter is added to control voltage dynamically [18] [19]. Furthermore, a selection of components is also included for USB type C applications.

4.2.1 CONSTANT ADJUSTMENT OF VOLTAGE

Many market-available voltage-regulators offer the possibility to select a desired constant output voltage following the configuration in Figure 17. These voltage regulators consist of built-in switches to perform step-down or/and step-up function.

Figure 17 represents the 2 pins that are relevant in order to adjust the voltage: the feedback pin and the output pin. The voltage at the feedback pin is set by a reference voltage V_{REF}, which is generated internally via an operation amplifier. By adding a resistor divider between the output voltage pin and ground, it is possible to adjust V_{OUT} following the formula in (1).

$$V_{OUT} = V_{FB} \cdot \frac{R_{BOT} + R_{TOP}}{R_{BOT}} \tag{1}$$
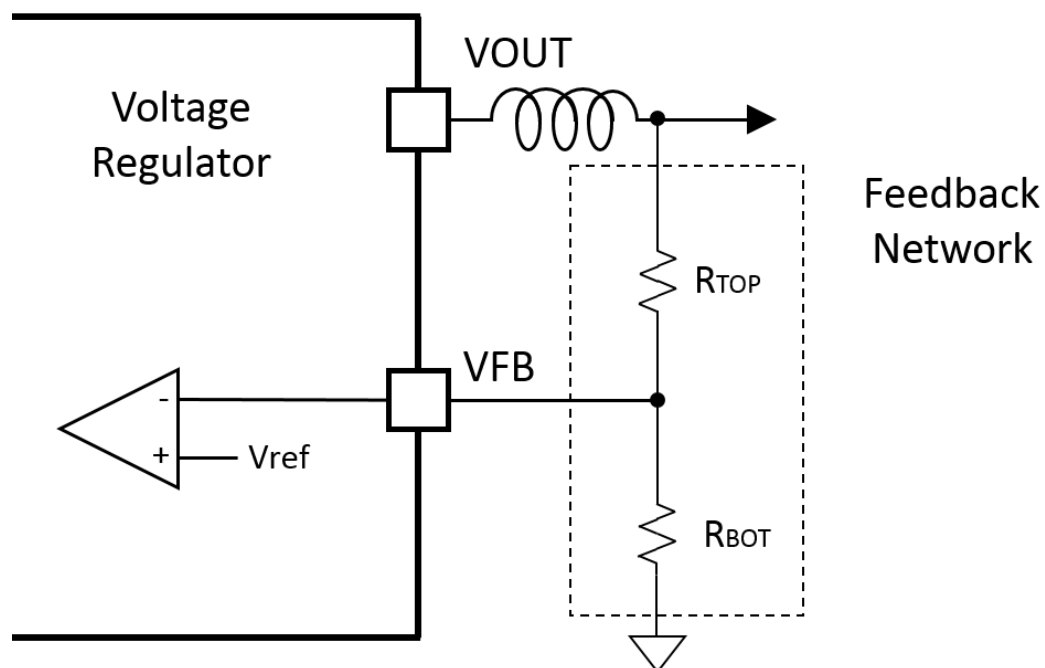
Figure 17: Circuit of a voltage regulator with constant voltage adjustment

While this approach is an effective and simple manner to control output voltage, it is not possible to adjust it dynamically. Hence this proves to be insufficient when working with USB type C given that it offers a wide voltage range from 5V to 20V.

4.2.2 DYNAMIC ADJUSTMENT OF VOLTAGE

By adding a DAC, it is possible to change the output voltage of the converter with the configuration presented in Figure 18. Now, 3 branches are connected to the feedback pin of the regulator which still has a voltage V_{REF}.

The output voltage can be defined as:

$$V_{OUT} = V_{ref} + i_{TOP} \cdot R_{TOP}$$

Based on Kirchhoff's law the sum of the currents is 0 given that the impedance of the operational amplifier is considered infinite.

$$i_{TOP} = i_{BOT} + i_{DAC} = \frac{V_{ref}}{R_{BOT}} + \frac{V_{ref} - V_{DAC}}{R_{DAC}}$$

Substituting this by the current flowing through the top resistor the output voltage is given by (2).

$$V_{OUT} = V_{ref} \cdot \left(1 + \frac{R_{TOP}}{R_{BOT}}\right) + R_{top} \cdot \left(\frac{V_{ref} - V_{DAC}}{R_{DAC}}\right) \tag{2}$$

If $V_{DAC} > V_{REF}$ the current flowing through the DAC resistor will be negative and will result in a lower output voltage. Similarly, when $V_{DAC} < V_{REF}$ the output voltage will increase.
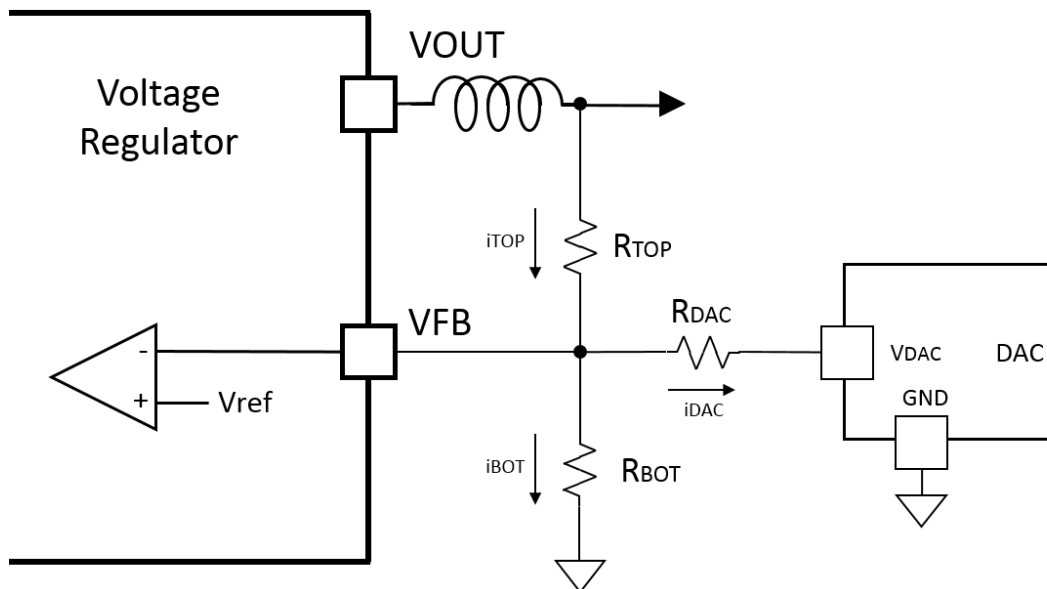
Figure 18: Circuit of a voltage regulator with dynamic voltage adjustment

4.2.3 SELECTION OF COMPONENTS

After analysing the theoretical operation of the circuits, this section includes the selection of components and calculation of resistor values for USB type C applications. Figure 17 shows 2 main components: voltage regulator and DAC. The following part numbers have been selected for the design following a criterion based on availability of product, cost-effective price and suitability for the application:

- Voltage regulator: *TPS5433* [20]. This step-down converter has an input voltage range from 5V to 28V which covers the entire voltage range of USB C. As for the current, the recommended output current is 3A which leads to a maximum output power of 60W per port.
- DAC: *DAC6574 [* [21]. This digital-to-analogue converter is controlled via the MCU through a I²C communication.

Kirchhoff's law is applied in the circuit shown in (3).

$$\frac{V_{REF} - V_{OUT}}{R_{TOP}} + \frac{V_{REF} - V_{DAC}}{R_{DAC}} + \frac{V_{REF}}{R_{BOT}} = 0 \tag{3}$$

By isolating *V$_{OUT}$* the equation becomes as follows:

$$V_{OUT} = R_{TOP} \cdot \left(\frac{V_{REF} - V_{DAC}}{R_{DAC}} + \frac{V_{REF}}{R_{BOT}} \right) + V_{REF} \tag{4}$$
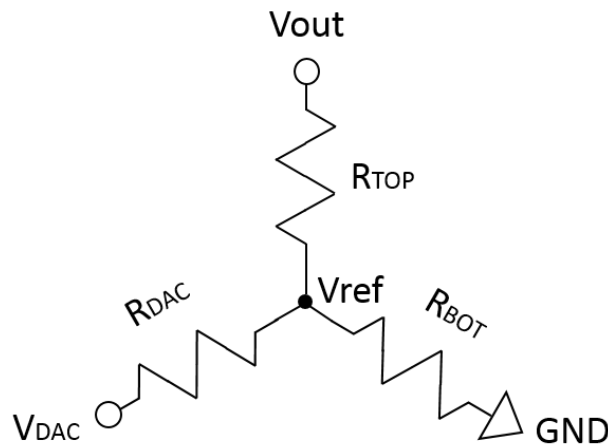
Figure 19: Circuit to apply Kirchhoff's law and calculate resistor values

As it has been stated previously, a lower DAC voltage results into a higher output voltage, which means these 2 parameters have an inverse relation. Given the voltage within USB C connectors ranges from 5V to 20V so the following logic is taken as criteria:

- When *V$_{DAC}$=0V* then *V$_{OUT}$=20V*
- When *V$_{DAC}$=3.3V* then *V$_{OUT}$=5V*

The reason why the maximum voltage level of the DAC has been set to 3.3V is due to the fact that this is a standard supply value for MCUs, ADCs and operational amplifiers among others. It is also known from the converter datasheet [20] that the reference voltage is 0.8V. Given that there are 3 variables and 2 equations the following relations are created:

$$R'_{BOT} = \frac{R_{BOT}}{R_{TOP}} \; \& \; R'_{DAC} = \frac{R_{DAC}}{R_{TOP}}$$

This results in 2 equations with 2 variables:

- $20 = \frac{0.8}{R'_{DAC}} + \frac{0.8}{R'_{BOT}} + 0.8$
- $5 = \frac{0.8 - 3.3}{R'_{DAC}} + \frac{0.8}{R'_{BOT}} + 0.8$

Solving this equation system results in the following proportion between resistors:

- $R'_{BOT} = \frac{R_{BOT}}{R_{TOP}} = \frac{33}{622}$
- $R'_{DAC} = \frac{R_{DAC}}{R_{TOP}} = \frac{3.3}{17}$

Given that the system still consists of 3 variables and 2 equations, a standard resistance value is selected for the top resistor: $R_{TOP} = 100k\Omega$. This value has been chosen due to high availability. Once this variable is known the other 2 resistors have been chosen: $R_{BOT} = 5.1k\Omega$ and $R_{DAC} = 18k\Omega$.

Given that the proportions between the resistors are not exactly the same as calculated for R'_{BOT} and R'_{DAC}, the maximum and minimum output voltages have changed:

- $V_{OUT_{MAX}}(V_{ADC} = 0) = 100 \cdot \left(\frac{0.8}{18} + \frac{0.8}{5.1} \right) + 0.8 = 20.93V$
- $V_{OT_{MIN}}(V_{ADC} = 3.3) = 100 \cdot \left(\frac{0.8 - 3.3}{18} + \frac{0.8}{5.1} \right) + 0.8 = 2.6V$

4.3 CURRENT ADJUSTMENT

The second parameter to be adjusted is the current. Being able to control the current provides the converter with an added value: it is possible to limit the current provided by each of the ports based on the number of loads connected or to charge the batteries in CC mode. In order to achieve accurate current measurement and control, 2 operational amplifiers are added as shown in Figure 20.

4.3.1 CURRENT MEASUREMENT: LOW PASS FILTER

The first step to limit the current is to measure the actual current that is flowing through the power path. The power path is represented by the thicker vertical line, the output current of the converter will flow through the shunt resistor which will have a voltage drop proportional to the current.

The purpose of the first operational amplifier is to act as a low-pass filter. [22] A low pass filter is an electrical circuit that is used to remove a desired range of frequency components. By implementing a low-pass-filter the high-frequency noise of the measured voltage drop is filtered and an accurate measurement is achieved.
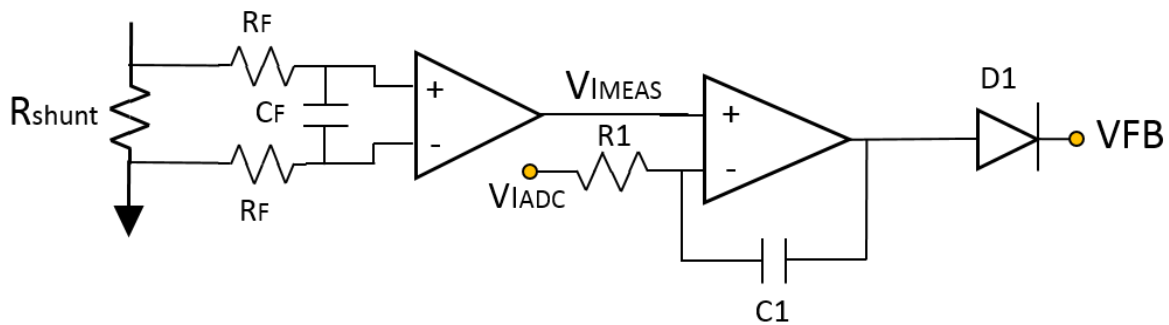
Figure 20: Circuit of current measurement and adjustment with 2 operational amplifiers

The values of the elements R_F and C_F are determined based on the formula (5) which determines the threshold value of the frequency. This means that any component with a frequency higher than $F_{threshold}$ will be filtered.

$$F_{threshold} = \frac{1}{2\pi \cdot (2 \cdot R_F) \cdot C_F} \tag{5}$$

For this design the frequency threshold has been set to 1.7 kHz by using standard values of the components: $R_F = 10\Omega$ and $C_F = 4.7\mu F$. It is assumed that the impedance of the operational amplifier inputs is infinite and therefore the R_F resistors are in series.

For the first operational amplifier an *INA 2181* [23] dual is chosen. This component offers different values of output voltage gains. In order to select the most suitable gain, it is helpful to pay attention to equation (6) which gives the voltage on the output of the first operational amplifier:

$$V_{I_{MEAS}} = I_{OUT} \cdot R_{SHUNT} \cdot Gain + V_{OFFSET} \tag{6}$$

The *INA 2181* has an offset pin in which a reference voltage can be applied which is added to the input signals. The purpose of this offset is to be able to measure current in both senses. Given that the supply voltage of the circuit components has been set to 3.3V, this offset voltage should be in the middle of this value so the same current can be measured in each direction, hence $V_{OFFSET}=1.65V$.

While the converter where this current control is implemented is unidirectional in the case of the charging station, when designing the circuit, the option for bidirectional current control was implemented given that this does not require more elements and the module can be used for other applications.

The output current of the port is limited by the converter. The datasheet of the *TPS5433* states that the maximum recommended current that the converter can supply is 3A. This means that when $I_{OUT}=3A$ the voltage on the output of the first operational amplifier should be lower than the supply voltage: $VI_{MEAS}<3.3V$. A trade-off between keeping the voltage levels within the limits and taking advantage of the measuring range and hence maximize resolution, the following selection has been made: $R_{SHUNT}=10m\Omega$ and *Gain=50V/V*.

- $VI_{MEAS_{MAX}} = 3 \cdot 0.01\Omega \cdot 50 + 1.65 = 3.15V$
- $VI_{MEAS_{MIN}} = -3 \cdot 0.01\Omega \cdot 50 + 1.65 = 0.15V$

4.3.2 CURRENT LIMITING: INTEGRATOR CIRCUIT

Once the current is measured and filtered, this signal is taken to the non-inverting input of a second operational amplifier which acts as an integrator as shown in Figure 20. The measured value VI_{MEAS} is compared to a reference value coming from the ADC, VI_{ADC} which is fed into the inverting input. If the difference between the 2 signals is positive ($VI_{MEAS}> VI_{ADC}$) this means that the load current has increased beyond its setpoint (normally limited by VI_{ADC}). In this situation the output of the integrator becomes positive and the diode *D1* is forward biased [24].

As illustrated in Figure 20, when current exceeds the set point, the integrator will send a current through the diode into the feedback pin of the converter. This current will flow through R_{BOT} increasing the voltage drop through the resistor and therefore increasing the feedback pin voltage. By sensing that the feedback pin voltage is over the reference 1.25V limit, the converter will decrease the output voltage in an attempt to decrease the current.

In order to find the relation between the output current limit and the reference signal coming from the digital to analogue converter, it can be assumed that the impedance of the operational amplifiers is infinite and therefore the voltage at the inverting and non-inverting pins is the same. Hence based on equation **(7)** the current limit can be isolated with the DAC signal as a variable:

$$I_{OUT_{LIM}} = \frac{V_{I_{DAC}} - V_{OFFSET}}{R_{SHUNT} \cdot Gain} \tag{7}$$

4.4 COMPLETE CIRCUIT

The complete circuit is illustrated in Figure 21 which consists of both voltage adjustment circuit and current limitation circuit. Voltage control is performed via the V_{DAC} pin highlighted in green, this adjustment is rather straightforward as it is directly connected to the feedback pin of the converter with a resistor.

The current limitation circuit consists of more steps: current measurement, filtering of this measured value and comparison with the reference value VI_{DAC} highlighted in yellow. This is also connected to the feedback pin of the converter via a diode that will only be forward biased when current needs to be limited.

The outcome of this circuit is the same operation as a commercial power supply: voltage setpoint and current limit are selected according to the application, if the current exceeds the limit given the load, then the voltage will be decreased until measured current equals setpoint.
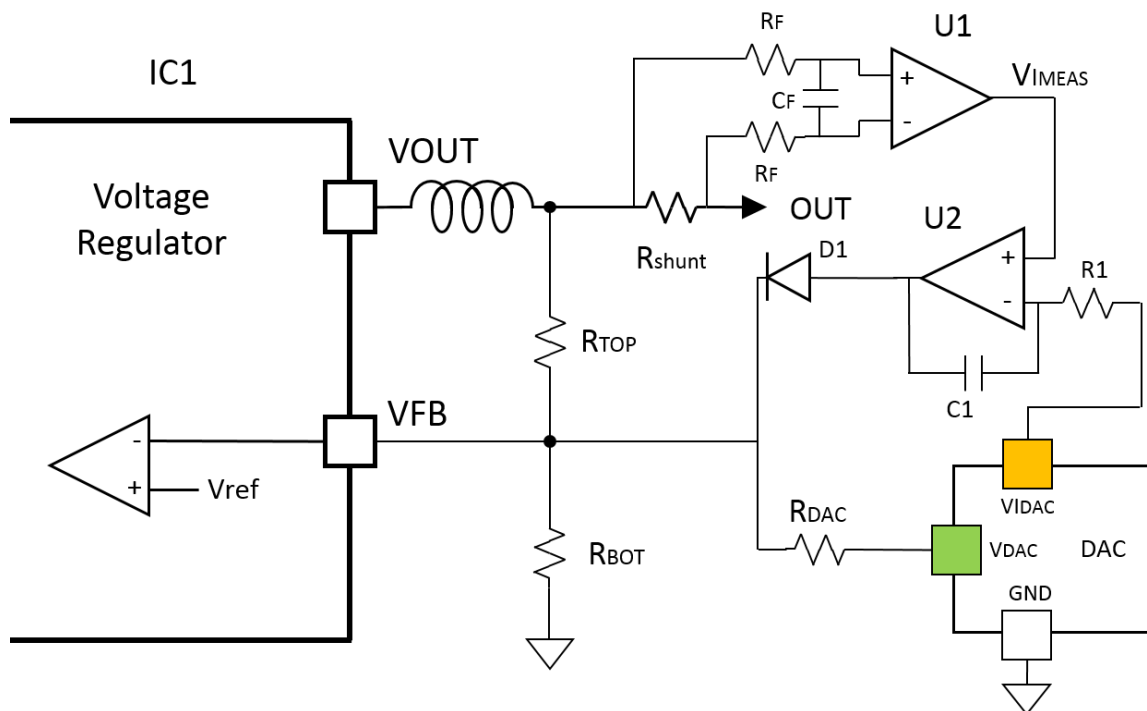
Figure 21: Complete circuit of dynamic voltage & current adjustment

The values and part numbers of the components used in this application can be found in Table 3. For the selection of the components within the second operational amplifier, a stability analysis was performed with the following criterion: achieve stability and small delay in current limitation activation time.

Table 3: Vales and part numbers of the components in the dynamic voltage and current adjustment circuit

Component	Value	Component	Value
R_{TOP}	$100\ k\Omega$	C_F	$4.7 \mu F$
R_{BOT}	$5.1\ k\Omega$	C_1	$330\ nF$
R_{DAC}	$18\ k\Omega$	D_1	MMDL914T3G
R_{SHUNT}	$10\ m\Omega$	U_1	INA2181
R_F	$10\ \Omega$	U_2	LM38DR
R_1	$1\ k\Omega$	IC_1	*TPS5433*

4.5 SIMULATION

After analysing the theory behind the voltage and current adjustment and making a selection of components, the next step is to carry out simulations with the purpose of validating the design. For this, the circuit has been implemented in the circuit simulation software TI-Tina [25] as shown in Figure 22.
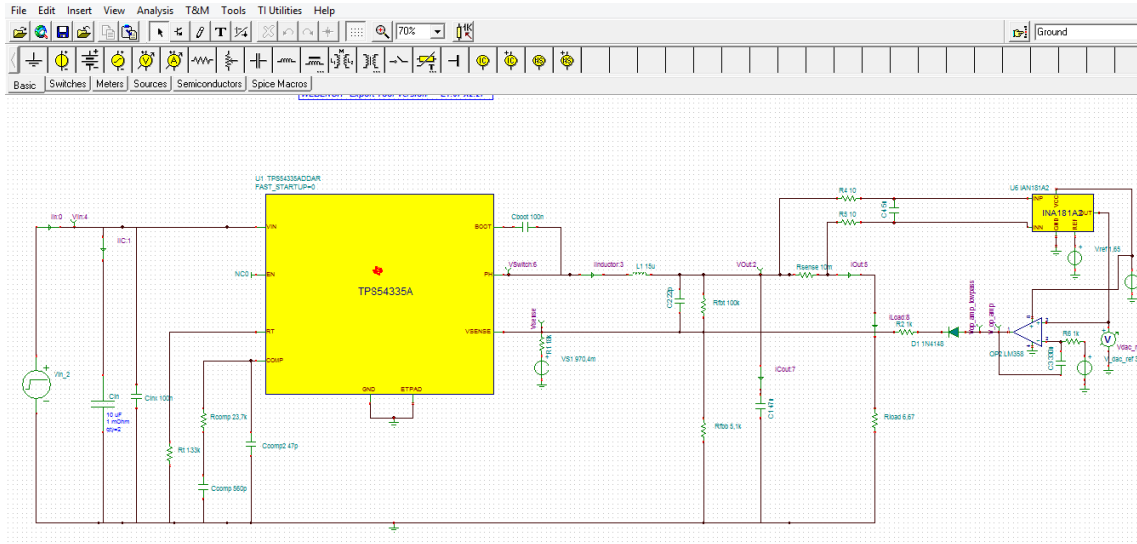
Figure 22: TINA-TI file simulating dynamic adjustment of voltage and current

The most relevant and challenging operating point of the circuit is when current limitation is active. In order to accomplish this, the following parameters have been selected for a 20Ω load:

- Vout is intended to be set at 20V and based on the formula (4) the equivalent V_{VDAC} is 0.25V
- Iout is limited to 0.5A and based on the formula (7) the equivalent V_{IDAC} is 1.88V.

The results of output voltage and current are depicted on Figure 23. Given that the load is purely resistive, the voltage and current are proportional and after an initial transient peak is hit, current is settled at 0.5A and consequently voltage adopts a value of 10V.
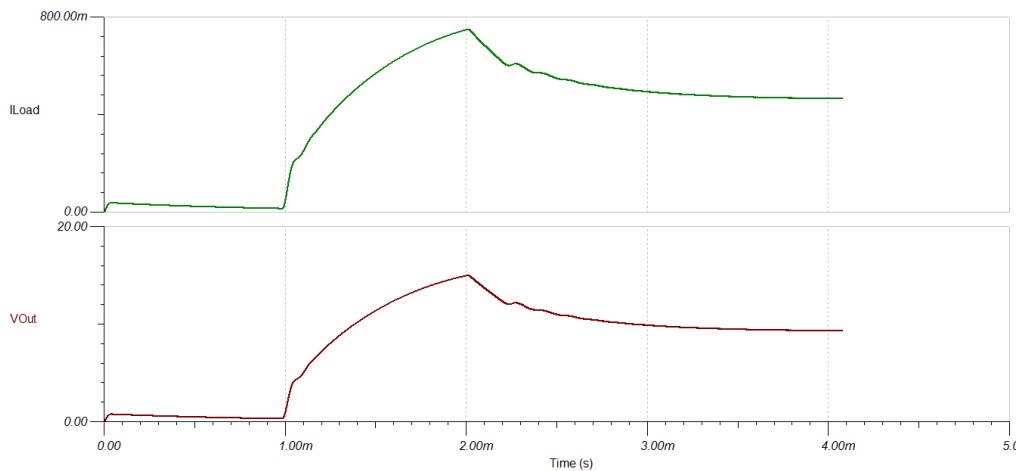
Figure 23: Output voltage and current results of the TINA-TI simulation

4.6 IMPLEMENTATION & EMPIRICAL RESULTS

After designing the circuits and running various simulation, the final step is to implement the dynamic adjustment of voltage and current in the solar charging station, which is discussed in this chapter. The section also includes a description on how the tests have been carried out as well as a discussion on the obtained results.

4.6.1 TEST SETUP & RESULTS

After building the charging station several tests were carried out with the purpose of implementing voltage and current dynamic adjustment and compare the empirical results to the theoretical formulas. The setup of the tests is shown in Figure 24. A power supply feeds 23V into the bus voltage of the charging station, which is also the input of the output port converters.

Figure 24: Charging station test setup in the lab

The microcontroller of the board is connected to a STM Nucleo [26] discovery board which enables communication with the software STM32 IDE [27]. With this setup, it is possible to flash the desired code to run the test. For this test, a load of 20Ω has been used and the operation has been divided into 3 intervals:

Table 4: Parameters of the 3 intervals within the dynamic voltage and current adjustment test

Interval	V_{VDAC} [V]	Equivalent V_{OUT} [V]	V_{IDAC} [V]	Equivalent I_{OUTLIM} [A]	Current limit
1	0.25	20	3.3	3.3	OFF
2	0.25	20	1.88	0.5	ON
3	3.3	1.8	3.3	3.3	OFF

For interval 1 the voltage is set to 20V (maximum of USB-C) and current limit is set to maximum, so it does not activate. For interval 2 the voltage is kept at the same level but current limit decreases to 0.5A which is not sufficient to have 20V with a 20Ω load, so current limitation is expected. Eventually, for interval 3 the voltage is set to the minimum with maximum current threshold, so no current limitation is expected.
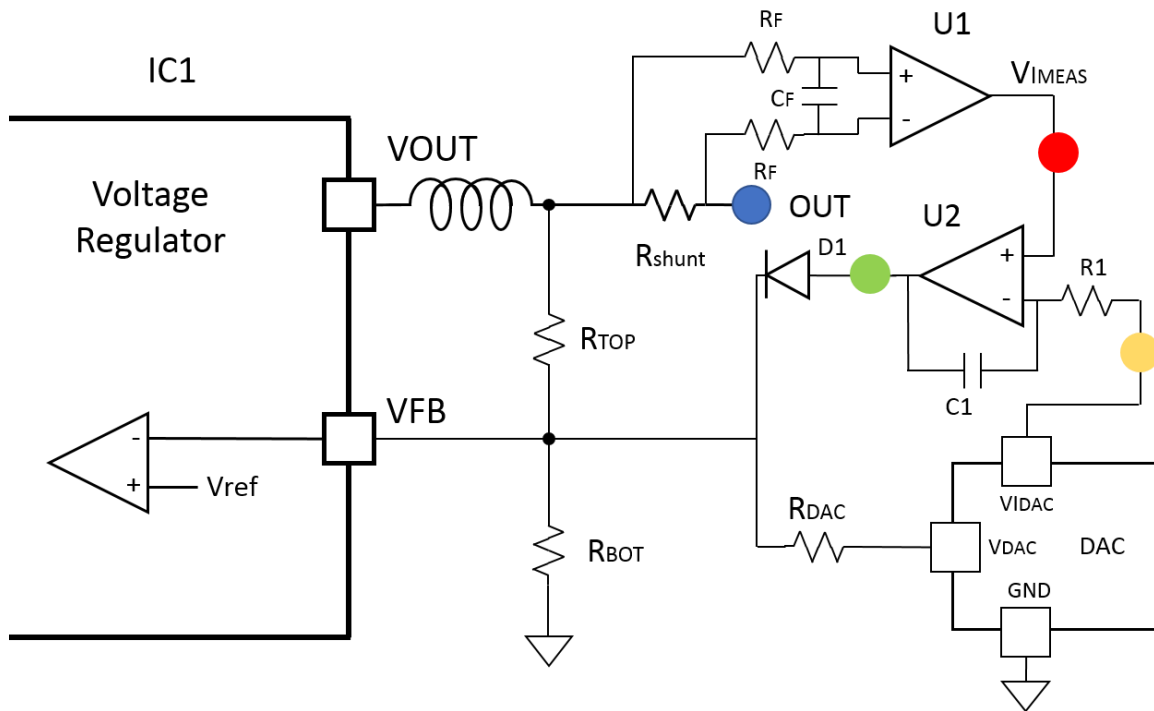
Figure 25: Measurement points highlighted with colours to indicate the location of the parameters in the circuit

Figure 25 shows the measurement points of the test highlighted in colour:

- Blue: output voltage
- Red: current measurement after low-pass filter
- Yellow: DAC current limit reference voltage
- Green: output of the current limitation circuit. A positive value indicates forward biased diode and active current control.

A) Interval 1

Figure 26 exhibits the shift from the operating mode in interval 1 to the operation of interval 2. During the first interval, the output voltage has been adjusted to be 20V which is represented by the blue line, this signal has a ripple of $\pm 0.8V$ with an average of 19.83V.

Current limit is set to maximum; this is represented by the yellow signal which has a value of 3.3V. The red line represents the current measurement and has a value of 2.132V, according to the formula of the current limit on (6), this translates to 0.964A. Given that the load has a resistance of 20Ω, this current fits the expected outcome.

The yellow and the red signals represent the 2 inputs of the second operational amplifier, red being the non-inverting one. Given that these 2 have the same scale on the oscilloscope, it is visually recognizable that since the red line is below the yellow one, current limitation should not be active. This is confirmed by the green signal which measures the output of the operational amplifier and oscillates around 0V.
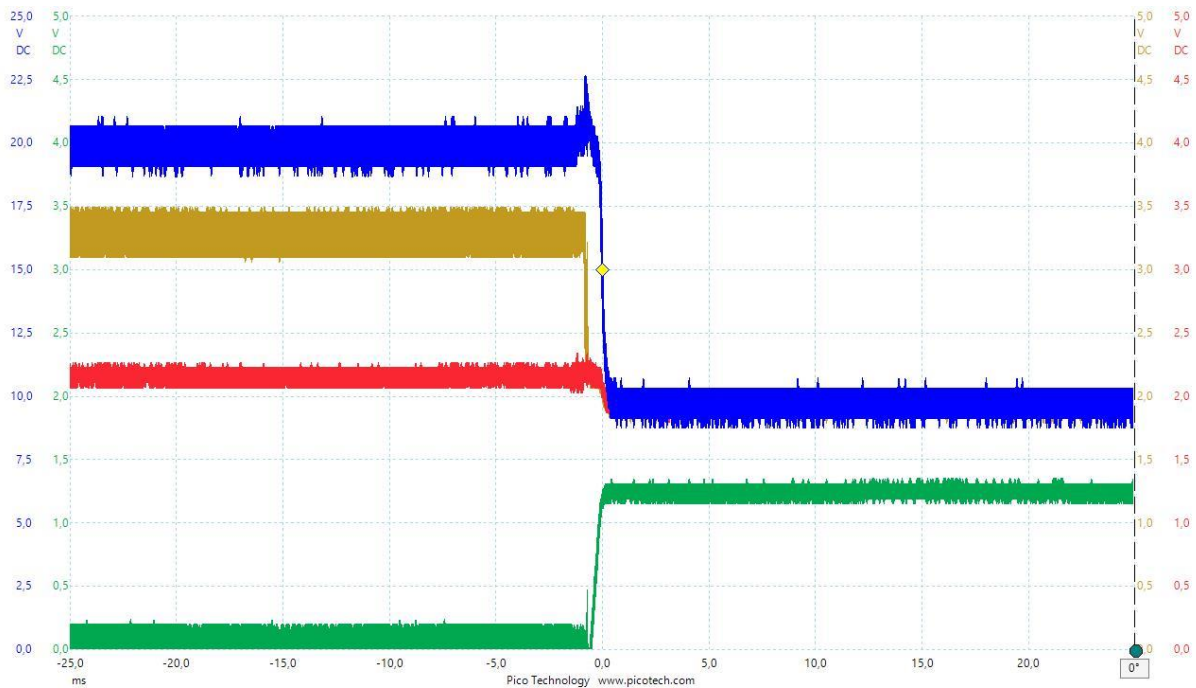
Figure 26: Oscilloscope results of the transition from interval 1 to 2

B) Interval 2

The operation of the second interval is present in the second half of Figure 26 and the first half of Figure 27. For this interval, the setpoint of output voltage is the same as for interval 1, 20V. However, the blue signal indicates that the output voltage is pulled down to 9.5V, this is an indicator of active current limitation operation.

Active current limitation is confirmed by the green signal, which is set high resulting in the current control diode D1 from Figure 25 being forward biased. Current will flow through this diode and this additional current will simultaneously flow through R_{BOT} resulting in a higher voltage drop through the resistor and hence decreasing the output voltage.

By decreasing the output voltage and given that the load is fully resistive, the output current will flow proportionally. This is represented by the red signal which decreases until it adopts the same value of the yellow line, the current limit setpoint.

In this case the current has been limited to 0.5A and based on the red signal which has an average value of 1.89V, the output current can be calculated:

$$I_{OUT\,LIM} = \frac{V_{I_{DAC}} - V_{OFFSET}}{R_{SHUNT} \cdot Gain} = \frac{1.89 - 1.65}{0.01 \cdot 50} = 0.48A$$

This result shows that there is a concordance between the measured voltage and current:

$$V_{OUT} = I_{OUT} \cdot R = 0.48A \cdot 20\Omega = 9.6V$$
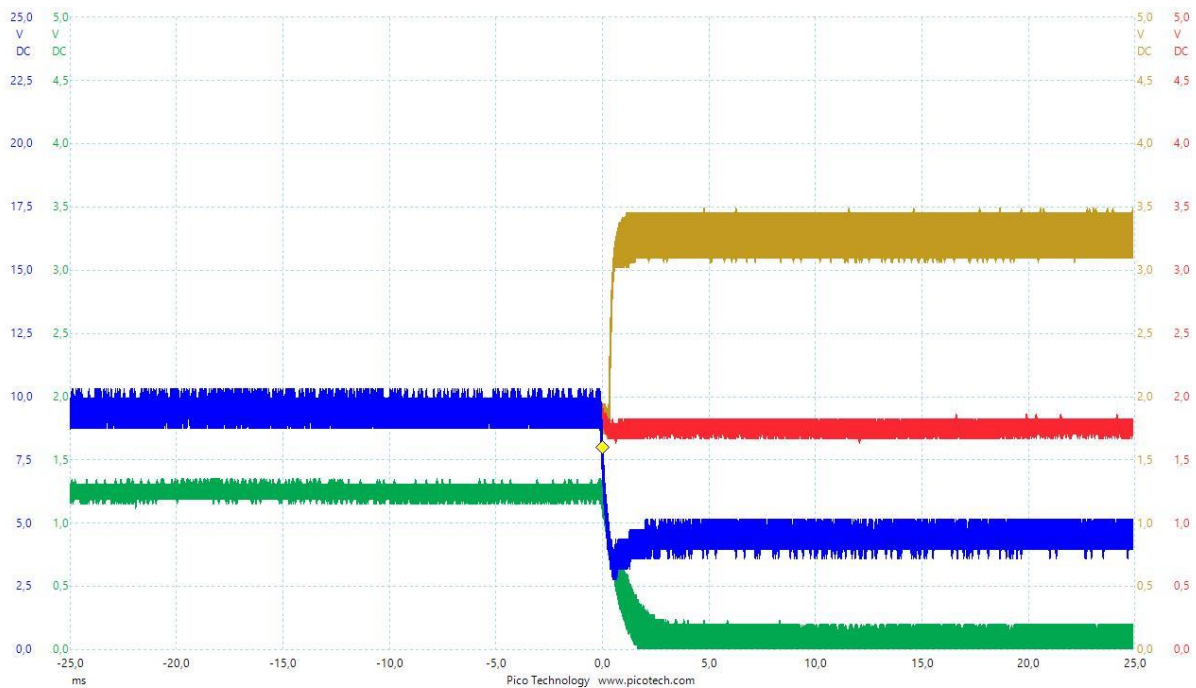
Figure 27: Oscilloscope results of the transition from interval 2 to 3

C) *Interval 3*

The operation of the last interval is present in the second half of Figure 27 and the first half ofFigure 28. For this interval, the setpoint of the output voltage is set to its minimum by giving a value of 3.3V to V_{VDAC}. Based on the blue line, this results in an output voltage of 4.4V

The current limit is set to its maximum as indicated by the yellow signal. Given that the voltage is minimum, no current limitation is expected. This is validated by the green signal which decreases to

an average value of 0V.A drop in output current can also be perceived by the red line as a result of the output voltage diminution.

Eventually, Figure 28 shows the transition from the interval 3 to the interval 1 described above. In this transition, the green signal is constant indicating that current control is not active for neither of the cases. Same pattern is followed by the yellow line which maintains a maximum current setpoint. The result is an increase of the output voltage represented by the blue line, proportional to an increase of the output current depicted in red.
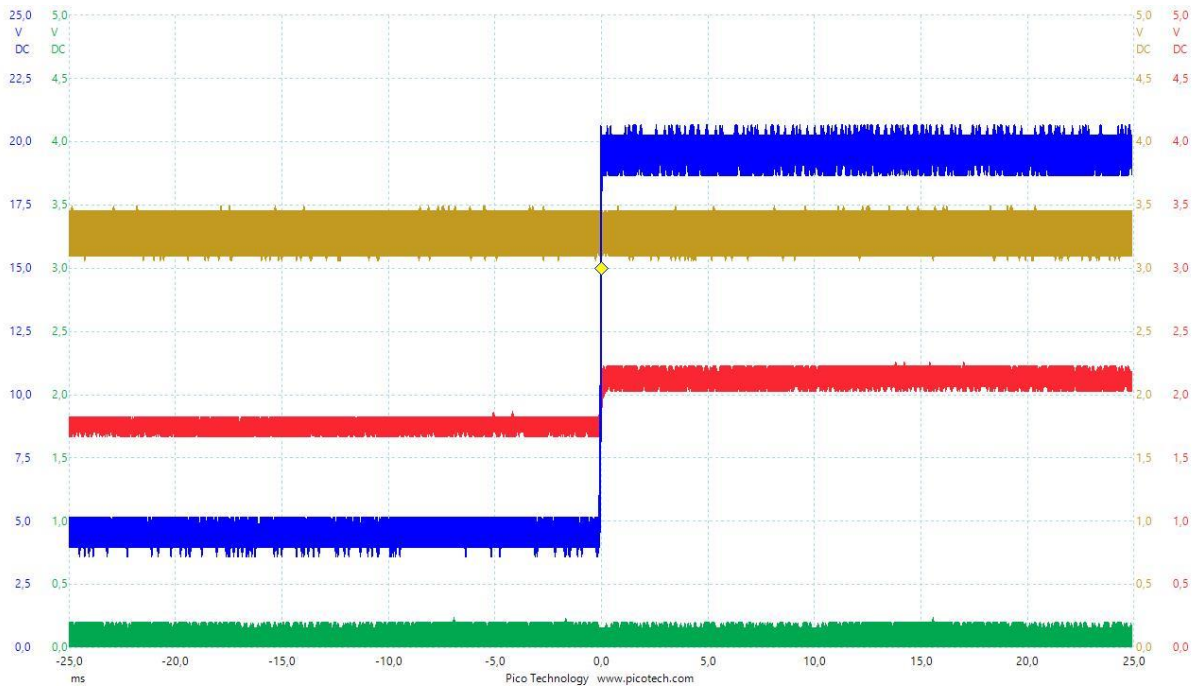
Figure 28: Oscilloscope results of the transition from interval 3 to 1

4.7 RESULTS COMPARISON & DISCUSSION

The aforementioned tests indicate a proper operation of the dynamic voltage & current adjustment for 3 points. However, it is important to analyse a wider range of operation to identify unexpected performances. Hence, the purpose of this last sub-chapter is to evaluate the operation of the design, compare it to the initial theoretical behaviour describes by circuit-theory, and comment on the results.

Several tests have been carried out with different voltage and current points and the results have been gathered in Figure 29. This figure consists of 2 plots: voltage and current. In each case, the vertical axis indicates the output values of the converter while the horizontal axis is destined for the signals coming from the digital-to-analogue converter.

As previously stated, the output voltage has an inversely proportional relation with the DAC. This is true for both empirical and theoretical values: the higher is the DAC value, the lower is the resulting output voltage. From the graph it can be deducted that the empirical results follow the theoretical tendency accurately. This is true specifically for the high output voltage range where the distance between both signals is the smallest. However, for higher DAC values (and therefore lower output voltages) the precision becomes lower.

As for the current, the DAC value is directly proportional to the output current. In Figure 29 the horizontal axis starts at 1.65V which is the offset value of the current measurement. While the current limiting circuit is designed to be installed in bidirectional applications, for this charging station power will flow in one directional only, therefore tests have been performed for positive currents only.
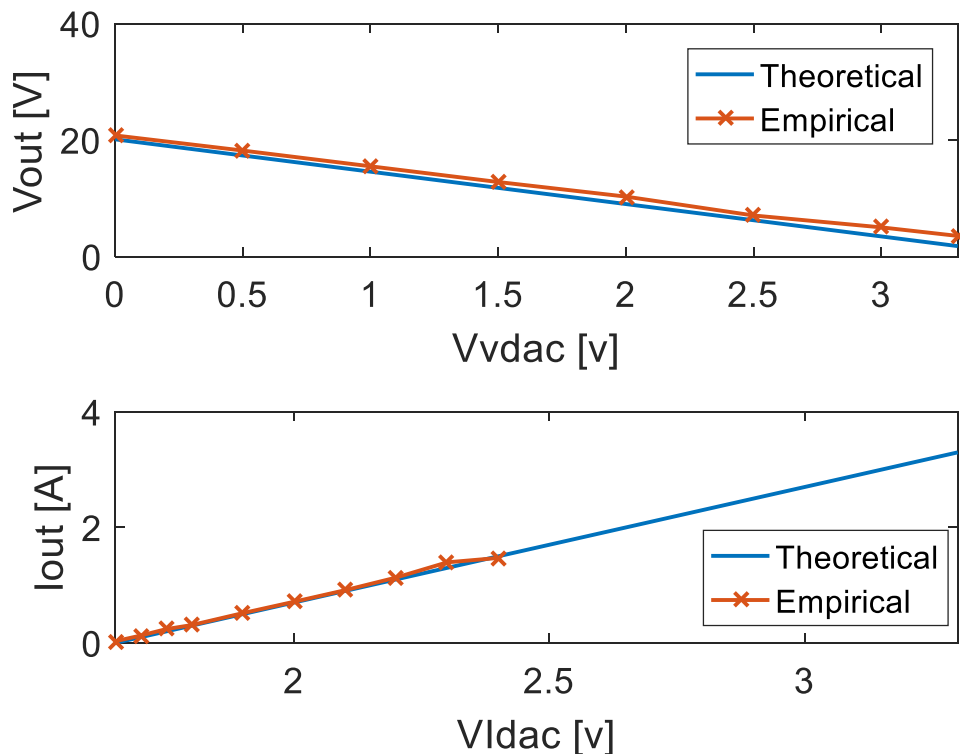
Figure 29: Comparison of theoretical and empirical results for output voltage and current

For both cases, the results are satisfactory given that the empirical behaviour assimilates the theoretical design. The results not only are satisfactory in the sense that they acquire the expected values but also that this happens rapidly. This is illustrated in Figure 26, where the measurement speed can be evaluated based on the blue and red signals which represent the output voltage and output current respectively. Voltage is measured directly so no delays can happen here but for the current, a low-pass filter is present for its measurement. This could cause a setback; nevertheless, this is not the case for this application though as both signals hit a peak and then proceed to stabilize at a lower value simultaneously. Based on this it can be concluded that the components (capacitors and resistor) of the low-pass filter meet the requirements as high frequency harmonics are filtered while providing a prompt and stable measurement.

Another critical point is the second operational amplifier of the current measurement circuit where the DAC signal is brought as an input. Again, based on Figure 26, the green signal indicates the activation of the current limitation. The period from the moment where the current setpoint (yellow signal) is updated to the moment where the green signal is stable is crucial. If this period is too long, it can damage the charging station. However, in this application the transition happens in less than 1ms.

In conclusion, the design proves to meet the design requirements satisfactorily. The charging station output converters can perform voltage and current dynamic adjustment in a reliable and cost-effective manner. It is effective and based on affordable components that lead to cheap mass production. This feature, together with the possibility of providing a maximum of 60W through 4 ports are key advantages for rural electrification projects.

5. CHAPTER

HIGH POWER-RATE POWER-BANK

After discussing the solar charging station, this chapter focuses on the second main component of the initial stages of electricity introduction: the high-power rate power-bank. As aforementioned, this element allows users to take electricity to their households as part of the SHS tailored for electrification of rural areas.

The chapter first presents the requirements that the power-bank should have leading to a design criterion. Based on this the design of the power-bank is explained in detail. It has been developed using the software KiCad EDA and consists in 2 PCBs positioned horizontally in parallel with 2 vertical connectors. These are divided into the upper PCB and the lower PCB. The chapter analyses each of the components, their functionalities and relevant information. It also includes both the layout design in KiCad and a picture of a physical of the prototype for both the upper and the lower PCB. This helps identify where each component is located within the PCB.

Eventually, a second revision of the power bank is also present in this chapter. While the main requirements are the same as for the first prototype, some updates are made based on the main criteria of offering a cost-effective product given that it is targeted for users with limited resources. In view of this, the power bank is reduced to a single PC, among other changes.

5.1 PURPOSE AND REQUIREMENTS

Portable energy storage plays a crucial role in the process of rural electrification: when in situ generation of electricity is not a viable option, users must be able to bring electricity to their homes by using for instance, power banks.

This practice is part of the initial stages of electrification as discussed in 3.2.2 At this point, users frequent a local shop where access to electricity is provided as a service by installing a solar charging station. Users utilize the power-bank as an interface to transport electricity from the shop to their homes by charging the battery cells. Later on, these cells are discharged in order to supply domestic loads.

Given that USB-C power delivery protocol is relatively new and in view of the limited market-available products, this chapter presents the design of a power-bank tailored for electrification applications. In order to carry out an initial design, it is important to list the desired features of the device:

- Cost-effective: the power-bank is intended to be used in low-income areas.
- Safe & reliable: operating with batteries entails a risk and since this power-bank is designed to be used in areas with unfavourable conditions, special attention is to be paid to safety.
- Fast charging: the power bank will be connected to the charging station while cells are being charged. Minimizing this time entails comfort for the user by decreasing waiting time and maximizing the potential of the charging station for the shop owner.
- High-power rate: being able to provide high-power outputs allows the user to connect a wide variety of loads as well as accelerating charging processes for mobile phones ,for instance.
- Various outputs: even though the power bank is a mobile device, when supplying domestic loads at home, some of these, such as lighting, will permanently be connected.
- Touch key sensors: capacitive touch key sensors are an alternative to conventional mechanical keys. Users can switch on/off and dim loads with this feature.
- Small: optimizing the volume in relation the storable capacity is important. Small volume and light weight are an added value when users transport the device frequently.
- Direct charging: being able to connect to the battery cells directly from the USB connector increases the efficiency by decreasing the number of converters involved. Furthermore, an innovative feature is that the cells can now be connected in series, resulting in lower currents and hence lower losses
- The power bank can power loads while it is being charged.

5.2 DESIGN OUTLINE

Based on the aforementioned requirements, the outline of the design of the power bank is presented in Figure 30. Energy is stored within the battery cells and these are directly connected to a battery management system which prevents the battery from operating outside its safe operating range. When the BMS is active the voltage level after it is the same as the battery bank and this is divided into 2 branches:

- Buck converter: this interface has a constant output voltage of 5V which is taken to ports 1,2 and 3. This power flow is unidirectional.
- Non-inverting Buck/Boost: this converter is the interface between port 0 and the BMS. The voltage level is controllable to fit specific applications and can provide up to 20V (maximum output of USB-C). This offers a wide input and output voltage range. The converter is bidirectional allowing battery charging from this port.

Port 3 also counts with a switch that directly connects the USB connector with the battery cells through the battery management system. Even though port 3 is connected only to the constant 5V converter, this switch plays an essential role to perform direct charging.
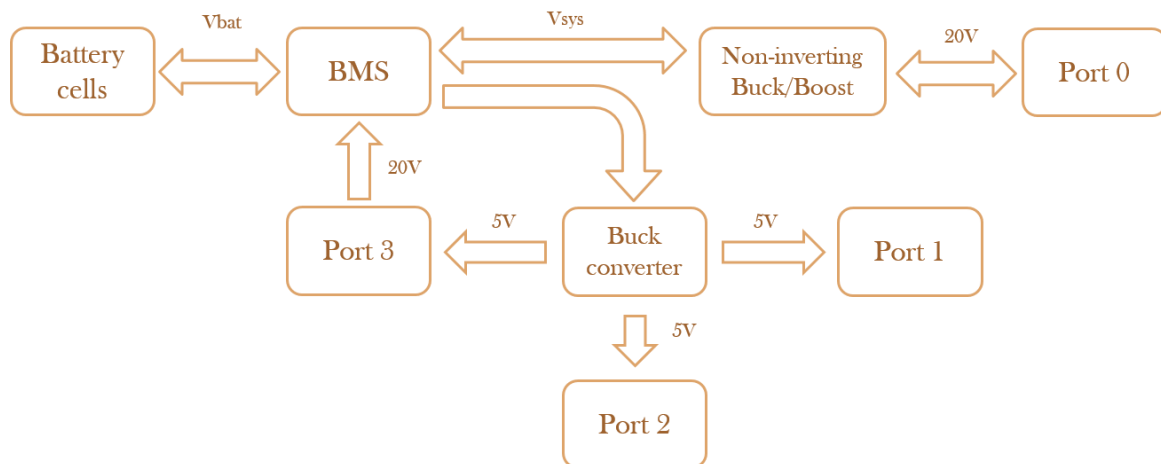
Figure 30: Block-diagram of the power-bank design

For this design each of the USB connectors can supply a maximum of 3A, this results in the numbers presented in Table 5 which summarizes the maximum input and output power of each of the ports based on their configuration.

Table 5: Summary of the rated output and input power per port of the power-bank

Port	Output power [W]	Input power [W]
0	60	60
1	15	-
2	15	-
3	15	60

5.3 2-LEVEL VERTICAL CONFIGURATION

As far as the dimensions of the power-bank are concerned, the battery cells will determine the size of the device to a big extent given that these will be the biggest components. The cells that have been used for this project are Samsung INR1865029E 2900mAh [28] and its dimensions are depicted in Figure 31. These cells have been chosen based on their capacity per unit of volume and charge/discharge properties.

Initially, a single PCB configuration was designed where all components were placed on the top and bottom layers of one circuit. This proved to be inefficient from a special perspective for 2 main reasons: firstly, given the 18.33mm diameter of the cells, this height is sufficient to fit 2 PCBs with corresponding components. Secondly, capacitive touch key sensors have been implemented and this feature requires avoiding vias in the area of the touch keys which makes the routing process challenging.

In view of the spatial problems that this could entail, a 2-level vertical configuration was opted for as depicted in Figure 31. In the sketch, 4 cells are connected in series occupying a total width of 73.2mm and 2 PCBs are placed in front of the cells coloured in blue and in green. The green PCB is denominated as the lower PCB while the blue one is the upper PCB based on their relative positioning. They are mechanically supported by each other via a vertical pin connector which also enables signal connections between the PCBs. This second revision optimizes the usage of space while ensuring a proper operation of the touch key sensors.
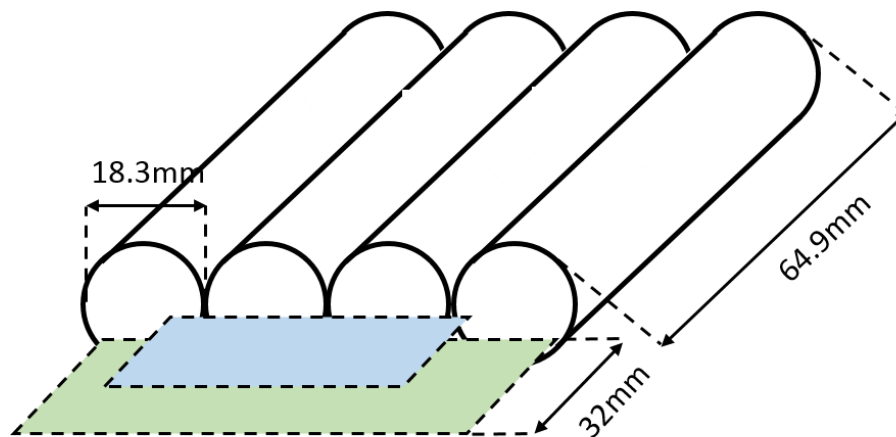
Figure 31: Visual representation of the cells with the PCBS in 2 level-configuration

The lower PCB is smaller than the upper PCB hence, this will determine the total length of the power bank. With a 32mm length the final dimensions of the power bank are 18.3mm height x 73.2mm width and 96.9mm length. As far as energy storage is concerned, given that the nominal capacity per cell is 2850mAh [28] and with a nominal voltage of 3.65V which results in a total energy of 41.61Wh.

These numbers satisfactorily meet the initial requirement of being able to have a high capacity in a small volume power bank.

5.4 UPPER PCB

Sections 5.4 & 5.5 include a detailed analysis of each of the PCBs layout, components, and operation. However, this chapter focuses on discussing the design criterion and functionalities of each of the elements that the power bank consists of.

The layout of the upper PCB is shown in Figure 32 which unlike the solar charging station, has been developed in KiCad, an open source electronic design automation software [29]. The PCB has a total width of 54mm and 27mm in length. It consists of 4 layers where components are placed on both the front and back layer of the board.
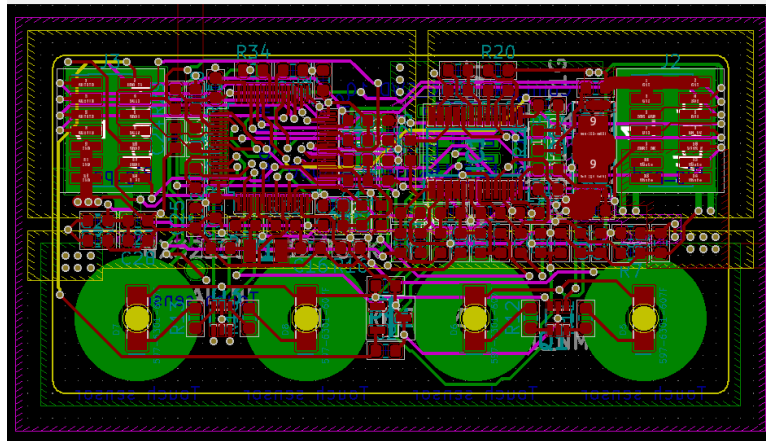
Figure 32: Layout of the upper PCB in KiCad

Figure 33 depicts a physical example of the upper PCB where the main components discussed in this chapter are highlighted: 1&2 vertical connectors, 3 MCU, 4 BMS and 5 LEDs and capacitive touch key sensors.
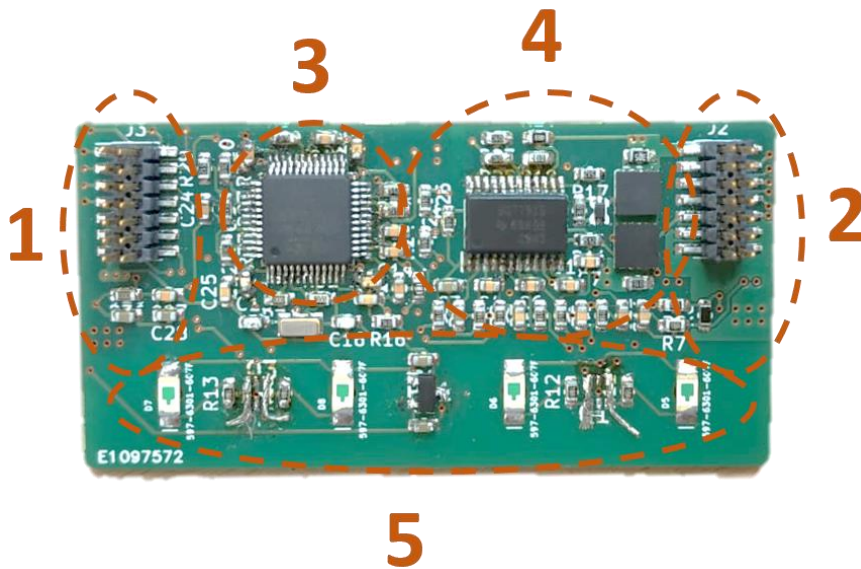
Figure 33: Prototype of upper PCB with highlighted elements

5.4.1 VERTICAL CONNECTORS

As previously discussed, the design of the power bank is based on a 2-level vertical configuration. The 2 boards are horizontally in parallel, and they are interconnected via 2 pin headers. These are symmetrically positioned, and each connector consists of 7 pins per row and a total of 2 rows. The connectors have 2 main purposes: mechanical support and electrical connection, signals are taken from one board to another via the pins.

5.4.2 MCU

The microcontroller used for governing the control of the power bank is an STM32. The reason behind this choice is based on various features: high availability, cost-effective prices, wide range of models with different memory densities, operating speeds and integrated features [30].

STM32 is the industry's largest family of microcontrollers and as a result, offers a variety of branches. For the power bank application, the most suitable series is the L0 which belongs the ultra-low power consumption branch. These MCUs offer the industry's lowest power consumption and this is a priority for energy storage devices.

In order to choose a specific MCU, it is important to pay attention to the features offered by each model in terms of pin functionalities: number of ADC, DAC, capacitive touch key sensors etc. Taking into account the analogue and digital signals present in the power bank circuit, the MCU used for the power bank is the STM32L072CBT.

The pin assignment has been carried out using the development platform STM32CubeIDE [31] as shown in Figure 34. The pins of the microcontroller include the following:

- Analogue measurements of voltage and current
- External clock
- LED indicators supply
- 2 I^2C communication channels
- JTAG connections for debugging
- Capacitive touch key sensors
- Port controller interfaces
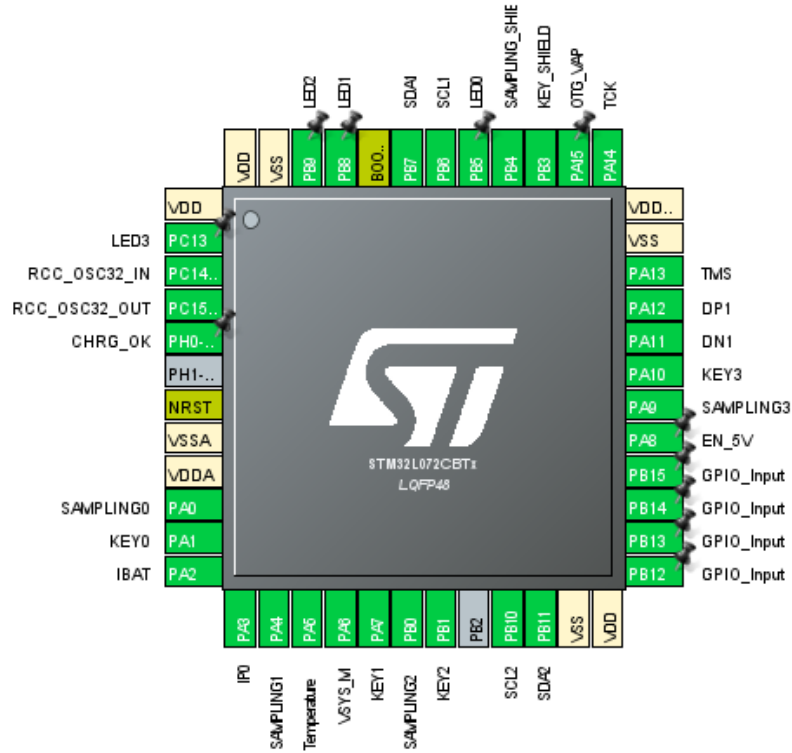
Figure 34: Pin assignment of the power-bank MCU in STM32 IDE

5.4.3 BATTERY MANAGEMENT SYSTEM

A BMS is an electronic system that has the purpose of ensuring a proper operation of the battery bank within its safe operating range. The functionalities of the batteries vary depending on the model, the most relevant being cell balancing to increase each cells longevity, monitoring its state and controlling the connection and the isolation of the battery bank based on protection measures. [32]

For this project an integrated circuit has been selected to perform the battery management, the BQ77915. This component has been chosen based on a combined criterion of suitability for a 4 series configuration and a low power consumption of $8\mu A$ under normal operation and $2\mu A$ under hibernate mode. [33]

The IC is a stand-alone component that does not require communication with the MCU. 2 external FETs are added to the system to govern charging and discharging of the battery bank as depicted in Figure 35. The BMS protects the cells from the following thresholds:

- Overvoltage: 16.8V
- Undervoltage: 11.6V
- Overtemperature during charge: 50ºC
- Overtemperature during discharge: 60ºC
- Overcurrent during charge: 8A
- Overcurrent during discharge: 6A
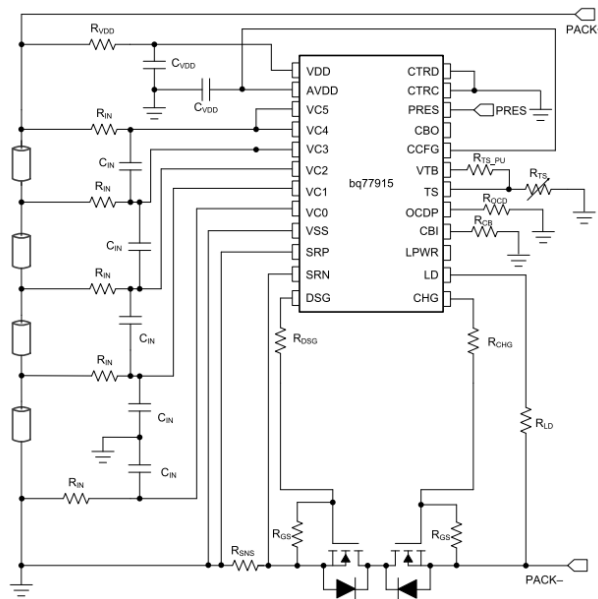
Figure 35: Typical application circuit of the battery management system datasheet [33]

5.4.4 CAPACITIVE TOUCH KEY SENSORS & LED INDICATORS

The PCB is equipped with capacitive touch-keys which enables user-interaction. The capacitance of a surface is measured via charge transfer acquisition, which is proven to be a robust and efficient method. The STM32 microcontrollers offer various I/O groups which consist of 4 pins each as shown in Figure 36. One of the GPIO is dedicated to sampling which is connected to ground via a capacitor (C_{Skey}). The other pins can be connected to electrodes via resistors (R_{Skey}) like in group 1. [34]
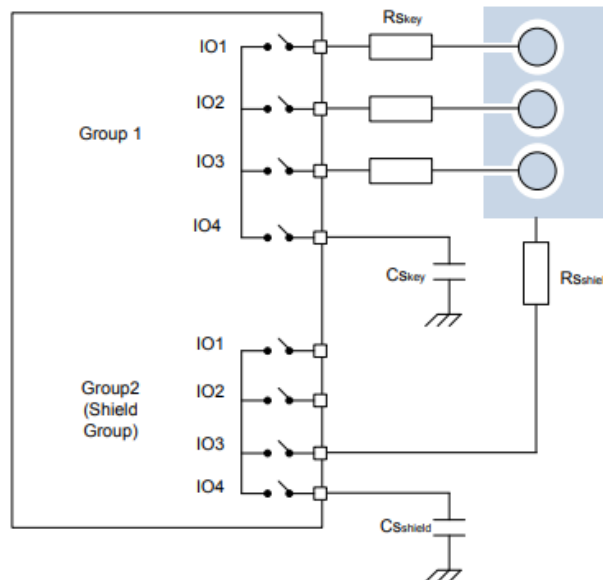
Figure 36: Typical application circuit of the capacitive touch key sensors [34]

When a finger is placed on top of one of the electrodes, its capacitance is altered. The principle of surface charge transfer acquisition lies on the transfer of the charge accumulated on the electrode into the sampling capacitor from the same group. Charge is transferred until a threshold is achieved and the number of transfers necessary to reach this limit varies depending on the electrode's capacitance, this is how a finger is detected. The charge within the electrode and the number cycles required to charge the sampling capacitor are inversely proportional.

One of the GPIO groups is dedicated to the shield which has the same structure as the electrode group. One pin is used for sampling while another pin is connected to the shield via a resistor, this shield is a surface around the electrodes. Utilizing a driven shield improves the sensitivity of the electrode given that the parasitic capacitance between the electrode and the shield does not need to be charged.

By including this feature, users can interact with the power bank by switching on/off specific ports or by controlling one of the loads such as dimming a light.

It is also important to monitor the operation of power-bank; hence LED indicators have been added on each of the ports to visually represent the state of each port or any other parameter such as the state of charge of the batteries. Given that no components can be placed on top of the electrodes, reverse-mount LEDs have been used as like the one shown in Figure 37. The lights are placed on the bottom layer of the PCB and light is directed towards the layers of the PCB. This light is transferred through a hole placed in the centre of the electrode. As a result, the keys where users place fingers will be lighted-up when a port is enabled.

Figure 37: Example of a reverse mount LED light [35]

5.5 LOWER PCB

The second part of the power bank is the lower PCB which contains the 4 outputs where loads are connected. With a length of 32mm and a width of 72.5mm, this PCB also consists of 4 layers, but components are only placed on the top layer. The design has been carried out in KiCad as shown in Figure 38 and a physical example is depicted in Figure 39.
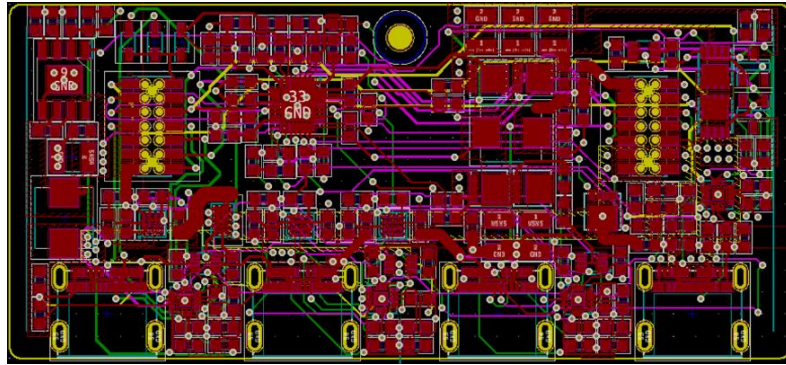
Figure 38: Layout of lower PCB in KiCad

The main components within the PCB are the following:

1. Port 0
2. Port 1
3. Port 2
4. Port 3
5. Buck converter
6. Non-inverting Buck/Boost converter
7. Buck/Boost driver
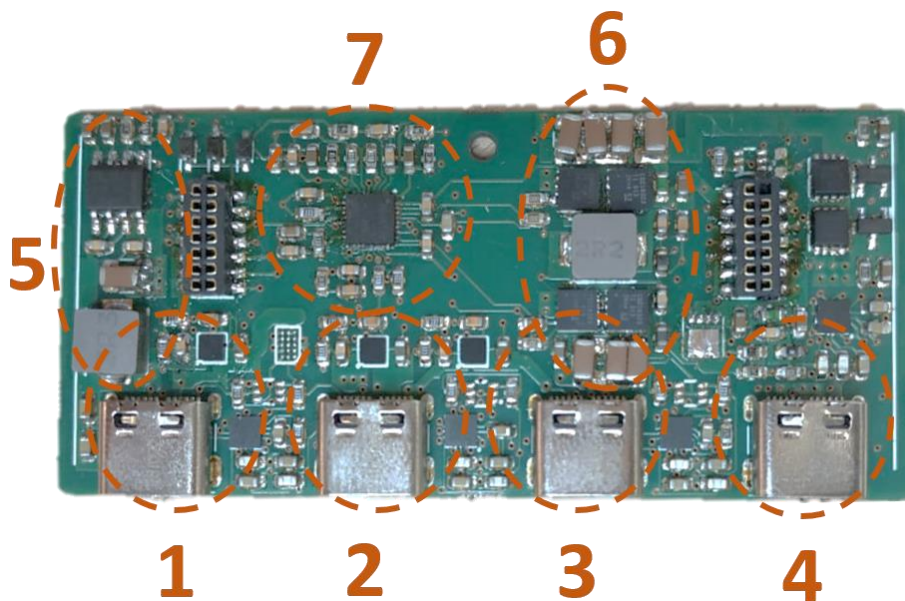
Figure 39: Prototype of lower PCB with highlighted elements

5.5.1 PORTS 1&2: LOW-POWER OUTPUT

The power bank consists of 4 ports ranging from port 0 to port 3 from left to right in Figure 39. Ports 1 & 2 are located in the central part of the PCB and both these ports have an identical structure depicted in Figure 40. The power path is represented by the colour-filled arrows and is unidirectional. The bus voltage coming from the cells is connected to a Buck converter with a constant 5V output. The interface between the output of the converter and the USB-C connector is a switch that is governed by a port controller which communicates to the microcontroller via I²C lines, these communication signals are represented with white arrows.
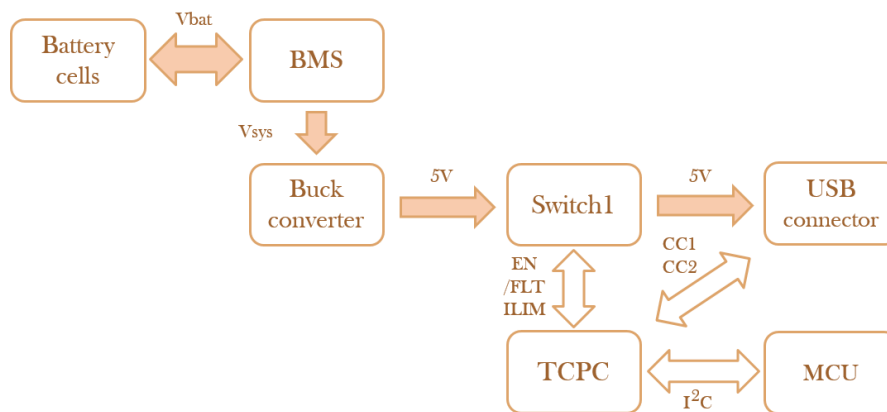
Figure 40: Block-diagram of ports 1&2 within the power-bank

A) *Buck converter*

For the Buck converter a TPS54628DDA IC has been selected based on its input and output voltage range and switching efficiency. The typical application circuit from the datasheet is shown in Figure 41. For this application the input voltage will be that of the battery cells and for the output a constant 5V is selected. In order to achieve this the values of resistor R1 and R2 have been calculated based on the formula (1). Regardless of the voltage within the cells, the output will be constant and this is connected to ports 0, 1 and 2. According to the datasheet of the converter, this can supply up to a maximum of 8.9A which is sufficient to have all 3 ports delivering maximum power with 3A each. The converter also has an enable pin which allows activation/deactivation of the switching activity through the microcontroller.
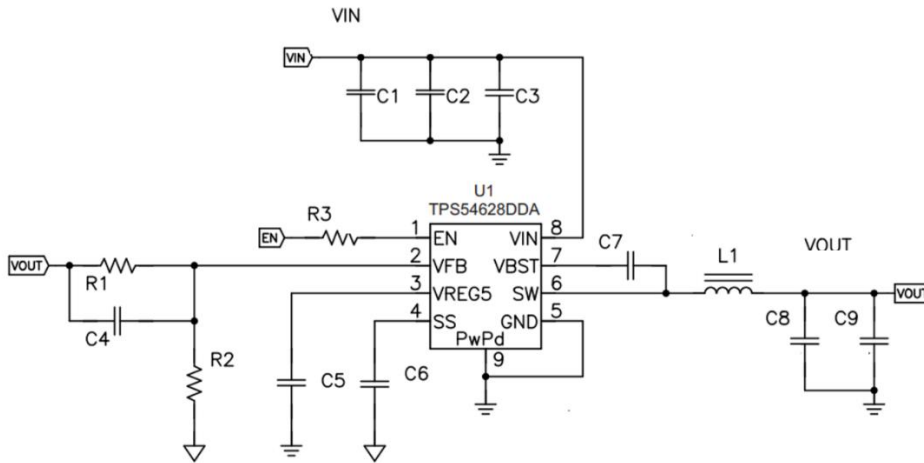
Figure 41: Typical application of the buck converter datasheet [36]

B) Port switch

Even though the 5V converter already has an enable pin which is controllable. This 5V power path is taken to 3 ports and by placing a switch between in all the ports, it is possible to control the delivery of power of each port individually. This provides safety by implementing protection such as overcurrent and overtemperature limits and it also enables giving priority to certain ports when the battery cells have a low SoC, for instance.

The switch utilized within the power bank ports is the *NX5P3290* [37] and its application diagram is depicted in Figure 42. The switch provides 2 main features that improve the operation of the port: adjustable current limit from 400mA to 3A via R_{ILIM} and overtemperature protection at 140 ℃.

Furthermore, 3 signals are connected to the port controller: an output fault signal (/FLT) that is activated to indicate that an overcurrent or overtemperature condition has occurred, an input enable signal (EN) from the port controller to enable the switch and an input fast turn on signal (FO) that allows reducing the power on inrush current. This last feature has not been used in the power bank application.
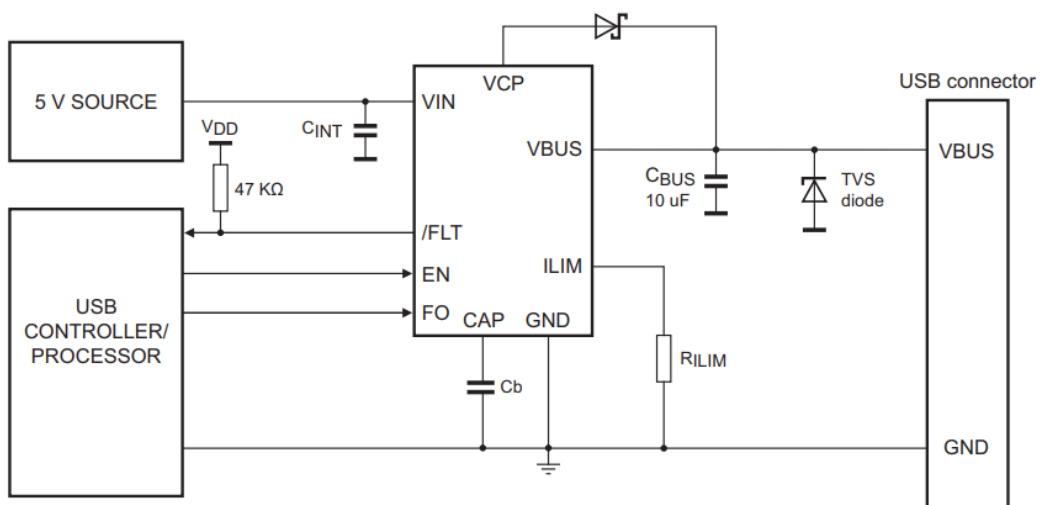
Figure 42: Typical application of the port switch datasheet [37]

C) *Port controller*

Working with USB type C requires a port controller that is compliant with USB Power Delivery and USB type C specifications. The *PTN5110* is the physical integrated circuit that fulfils this task in this project. These are the features provided by the port controller [38]:

- 2 power path enable controls: EN_SRC and EN_SNK. For ports 1 & 2 only one of this is used given that the power flow is unidirectional. However, for bidirectional ports 0 & 3 2 switches are implemented and each of this is individually controlled by these signals.
- The I^2C communication interface with the port manager (the MCU) enables status update. The PTN5110 allows up to a maximum of 4 addresses that enable the implementation of 4 ports in one I^2C line.
- As aforementioned, the switch offers a feature to select the current limit with the value of a resistor. On top of this, the PTN can dynamically adjust this limit depending on the circumstances.
- Another pin already explained in the switch section is the /FAULT pin which is read by the port controller to recognize any fault detected by the switch. Furthermore, the PTN5100 also is equipped with an ALERT pin connected to the port manager to inform about the fault status.
- The port controller is equipped with 2 channels CC1 and CC2 which manages the Source-to-Sink connection and data communication. These pins are connected to the USB connector and they are dedicated to the presence detection and orientation detection of a source or a sink. [39]

5.5.2 PORT 3: DIRECT CHARGING

The structure of port number 3 is similar to that of ports 1 and 2 with an added component: a second switch. This second switch, denominated Switch2 in Figure 43, directly connects the battery management system with the USB connector. This is a key element for direct charging as it enables providing power from the connector to the battery management system directly, without conversion.
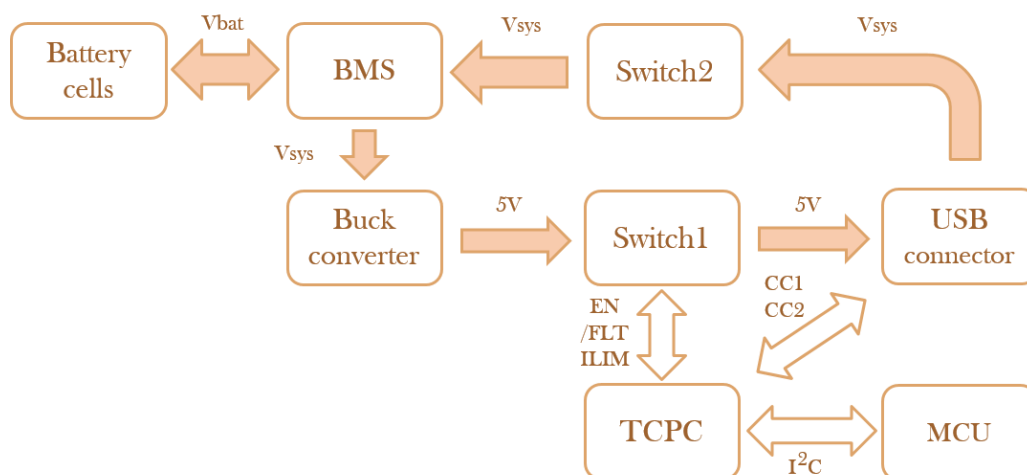
Figure 43: Block-diagram of the port 0 within the power-bank

Switch 1 remains the same in ports 1 & 2 but for Switch 2 another NXP variant has been utilized: *NX20P50900* [40]. While the operating principle of the switch is the same, this model allows a wider range of input voltage, from 2.5V to 20V. This is required that the voltage on this power path will be the same as the battery cells voltage. Given that 2 switches are present in this port, this can operate as both source and sink:

- When switch 1 is activated, the EN_SRC signal of the PTN is high and the power-bank takes the role of an energy source by providing 5V to the connector where a load is connected.
- When switch 2 is activated, the EN_SNK signal of the PTN is high and the power-bank takes the role of a load by charging the batteries.

5.5.3 PORT 0: BIDIRECTIONAL NON-INVERTING BUCK/BOOST

Port 0 has a different structure compared to the rest of the ports. This port connects the connector voltage of port 0 with Vsys via a non-inverting Buck/Boost converter depicted in Figure 44. This 4-switch converter is controlled via the *BQ25713* [41] battery charge controller.

This dedicated chip allows bidirectional power flow as well as selection of desired voltage on the connector together with many other features. When the battery is being discharged through this port, power flows from right to left in Figure 44. The first element is a P type MOSFET which is driven by the signal *BATDRVb* which separated the system voltage from the battery voltage. It provides UVLO protection when the battery is depleted.

Before going through the switch, the current flows through a shunt resistor and he voltage drop is measured by the *BQ25713,* these signals are represented by green tags. Current is measured in 2 instances, first at the battery cells side and the second one on the connector side. The charge controller prevents overcurrent and also provides current monitoring pins on input and output

4 orange signals drive the gates of the 4 switches within the converter, these will determine the voltage on the connector. Eventually 2 switches are connected in series to control charging and discharging.
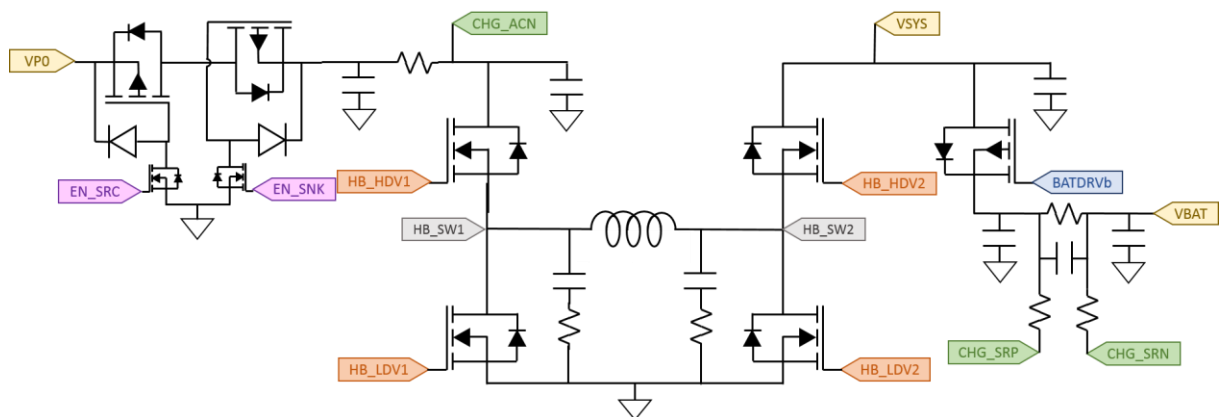
Figure 44: Representation of the Non-inverting Buck/Boost converter circuit

5.6 SECOND REVISION

After testing the first built revision of the power bank, various improvements were identified, and errors were fixed by designing a second iteration. Taking into account that the target users of this technology are villagers with limited resources, one of the main challenges is to keep the price low. In order to achieve this, the approach is to substitute costly dedicated chips with circuits developed for the project based and affordable elements such as passive elements (resistors, capacitors and inductors) and basic semiconductors such as MOSFETs.

5.6.1 DESIGN UPDATES

While the overall criterion presented in 5.1 is the same, some adjustments have been made for this second iteration:

- While the touch key sensors provide comfort to the user, this technology is intended to devices where loads are stationary. This is not the case of the power bank given that it will regularly be taken to be charged at the charging station. These elements entail an added cost and furthermore, they do not allow placing vias on the surfaces of the touch key sensors. This challenges the routing of the signals and requires more space within the PCB.
- Taking advantage of the extra space obtained by not using touch key sensors, another improvement is to avoid the 2-level configuration. While it is a convenient system to optimize space, the vertical connectors utilized to electrically connect and mechanically support the PCBs, add a significant value to the price. Consequently, the second revision only has 1 PCB.
- One of the most complete components of the first revision was the non-inverting Buck/Boost converter which enables bidirectional power flow and selection of voltage level. This converter is governed by a dedicated chip that is expensive and therefore this converter is not included in the second revision.
- Even though some components are not present anymore, the operation of the power bank and its functionalities should be the same. The purpose of the aforementioned converter was providing the option to connect sources with voltages lower than the batteries, to a connector and feed power into the battery cells. Therefore, in this second revision a Boost converter is included to meet this requirement. This boost converter counts with input current limitation controlled by the MCU, offering 3 values: 1.5A, 3A and 5A.
- While the MCU in this iteration is still a STM32, the series has been changed from L0 to G0. The reason behind this replacement is that the G0 family includes the peripherical and firmware for USB-C power delivery . As a result, there is no longer need to include port controllers for 2 of the ports. Furthermore, when the first revision was developed, this series had not been released yet. This saves space and also decreases the overall price of the power bank.

5.6.2 DESIGN OUTLINE

The updates implemented in the second version of the power-bank result in the block-diagram depicted in Figure 45. The battery bank is directly connected to a BMS which can disconnect the cells from Vsys via a low-side switch if a fault occurs. When the BMS is on, the system voltage has the same value as the battery cells which have a nominal voltage of 14.6 V. The system voltage is divided into 2 branches, the first one is connected to a Buck converter which steps-down the voltage to constant 5V. This connection is taken to all 4 ports which count with a switch each. As a result, each port can be activated or deactivated depending on the operating conditions.

Ports 1, 2 & 3 are unidirectional and can provide output power up to 15W each with 5V and a maximum of 3 A. Port 0 offers more functionalities such as bidirectional power flow. This port is connected to a P type MOSFET that is controlled with the signal EN_CHRG by the MCU. This switch is ON if the battery cells are charging; however, this can be done in 2 manners: direct charging or with a boost converter.

If the power-bank is being charged with the solar charging station, the station has the possibility to adjust output voltage and limit the current. Hence, these parameters can be negotiated based on the cells state of charge and the power coming from port 0 can be directly fed into the battery without any conversion via direct charging. In this case, the signal EN_CHRG will be ON and the current will flow through the diode of the switch controlled by the signal EN_DSCHRG. For higher efficiency, this second switch can also be turned ON and make a direct connection between the system voltage and the port 0 voltage. This same path can be utilized to discharge the batteries and provide high-power to port 0 with power up to 50W (16.8 V and 3A).

The power bank also offers the possibility to charge with sources other than the solar charging station, this provides compatibility with a wide range of products. If a conventional USB cable is connected to port 0, it will provide 5V to the input of the Boost converter and this is stepped-up to the voltage of the battery cells.
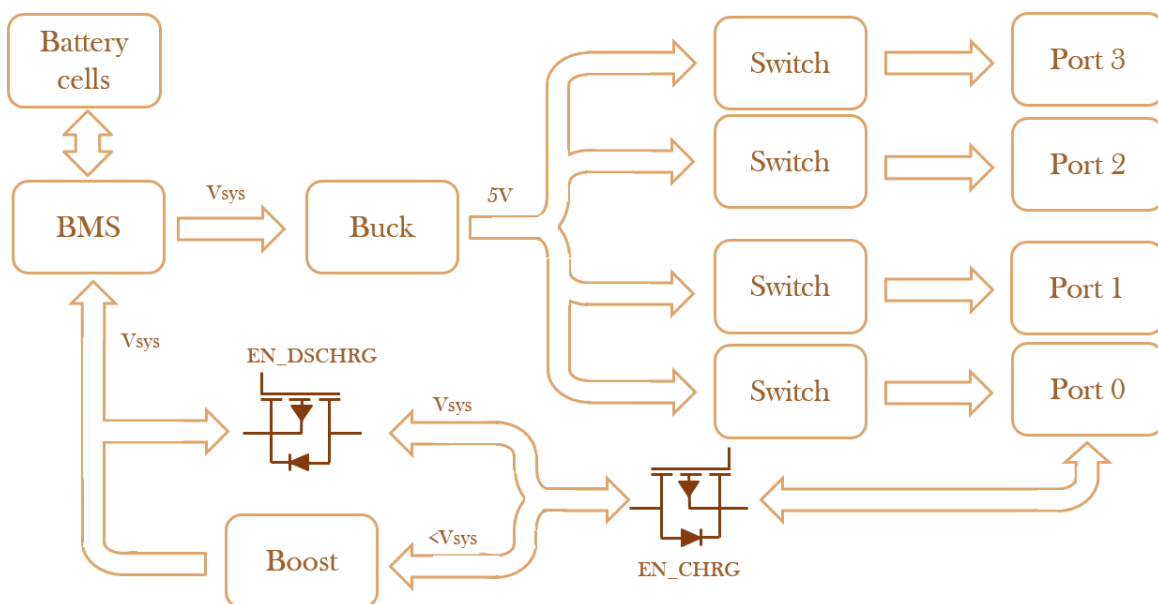
Figure 45: Block-diagram of the second revision of the power-bank

The layout of the second revision PCB is presented in Figure 46 and a prototype of the physical PCB is depicted by Figure 47. This design has also been developed with KiCad.
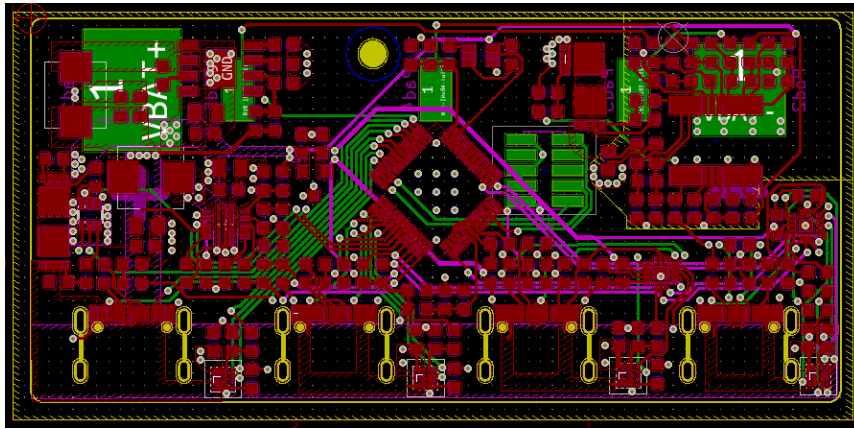
Figure 46: Layout of the power-bank second revision in KiCad

The main components that can be distinguished within the PCB are:

1. BMS
2. Buck converter
3. Boost converter
4. 2 switches for direct charging
5. MCU

Figure 47: Prototype of the power-bank second revision with highlighted elements

5.6.3 FINAL PRODUCT

After designing and building protypes, the PCBs were debugged and after proving proper operation these were connected to the battery cells resulting in the final product depicted in Figure 48. The picture shows the PCB fitted into a 3D printed case which consists of 2 parts. The PCB is positioned upside down and the connection pads for the battery cells are on top. 2 big pads are connected to the + and – of the 4 cells in series while the interconnections between the cells is also measured for the BMS.
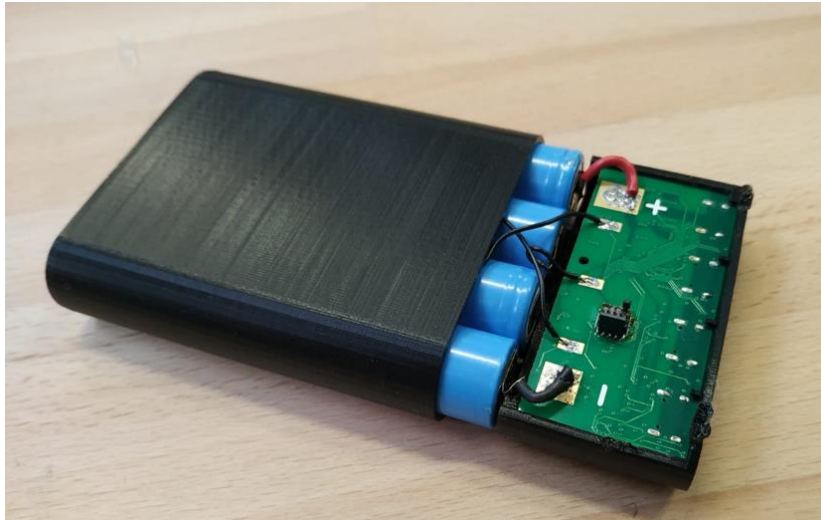
Figure 48: Working prototype of a 4-cell power-bank with 3D printed case

The prototype in Figure 48 shows a power-bank with 4 cells in series with 2850 mAh typical capacity and 3.65V as nominal voltage per cell. Given that they are connected in series the capacity is the same as per cell, but the nominal voltage rises to 14.6V which results in 41.61 Wh. The same PCB can be connected to battery banks with higher capacities but not higher voltages. This is the case of the bigger power-bank depicted in Figure 49 which consists of 8-cells where 4 clusters of 2 cells in parallel are connected in series with an energy storage potential of 83.22Wh. [28]

Figure 49: A 4-cell power-bank prototype on the left and an 8-cell prototype on the right

6. CHAPTER

BATTERY CHARGING

After analysing the solar charging station and the high power-rate power-bank, this chapter focuses on the interconnection of these 2 elements. This chapter includes the results obtained from the battery-charging test. Initially the setup of the test is explained in order to understand what parameters are measured and what is the intended outcome of their measurements. 2 tests are performed, even though both have the same goal, which is charging the battery, each follows a different approach: conventional USB charging and direct/fast charging.

For both cases results are presented in the form of graphs including battery voltage and current as well as power and energy. Furthermore, given that there are converters as part of their circuit, their switching patterns are analysed and discussed based on their topology.

The goal of this chapter is making a discussion on the comparison between 2 approaches. Hence, for both cases the most relevant parameters are obtained and compared to understand to what extent it is beneficial to use the USB-C and direct charging compared to the conventional USB.

6.1 TEST SETUP

This final test within the project involves the 2 main components analysed throughout the report: the solar charging station & the high power-rate power-bank. The test consists in charging the battery cells utilizing 2 different approaches: direct/fast charging and conventional USB charging. The purpose of the test is to collect data during the charging process in order to add a discussion on the results.

Both tests have the same starting point: the battery cells are depleted as a result of the under-voltage fault, the BMS opens the switches disconnecting the battery cells. The setup of the test is depicted by Figure 50: the solar charging station and the power-bank are connected via USB connection. In a real application environment, the power source would be a PV panel connected to the MPPT input. However, for this test a power supply has been utilized feeding power directly into the bus voltage of the charging station.

2 tests are performed, and the same parameters are measured in both tests with the goal of shedding some light on how much battery charging is improved compared to conventional USB charging.

Figure 50: Battery charging test setup

6.1 DIRECT CHARGING

For the first test the output of the charging station is set to 16.7V. This value is selected based on the battery cells datasheet [28] which defines the charging voltage of each cell at 4.2V. Fort this prototype 4 cells are connected in series which results in an overall voltage of 16.8V. The current limit is set to its maximum, 3A.

Figure 51 represents the diagram of the power flow within the test. The power source is an external power supply that is directly fed into the bus voltage of the charging station. Even though the converter is configured to supply 16.7V, it is directly connected to the battery cells, hence it will adopt the same voltage level. As a result, the power will flow through the direct charging module within the power bank as represented by the coloured arrows.
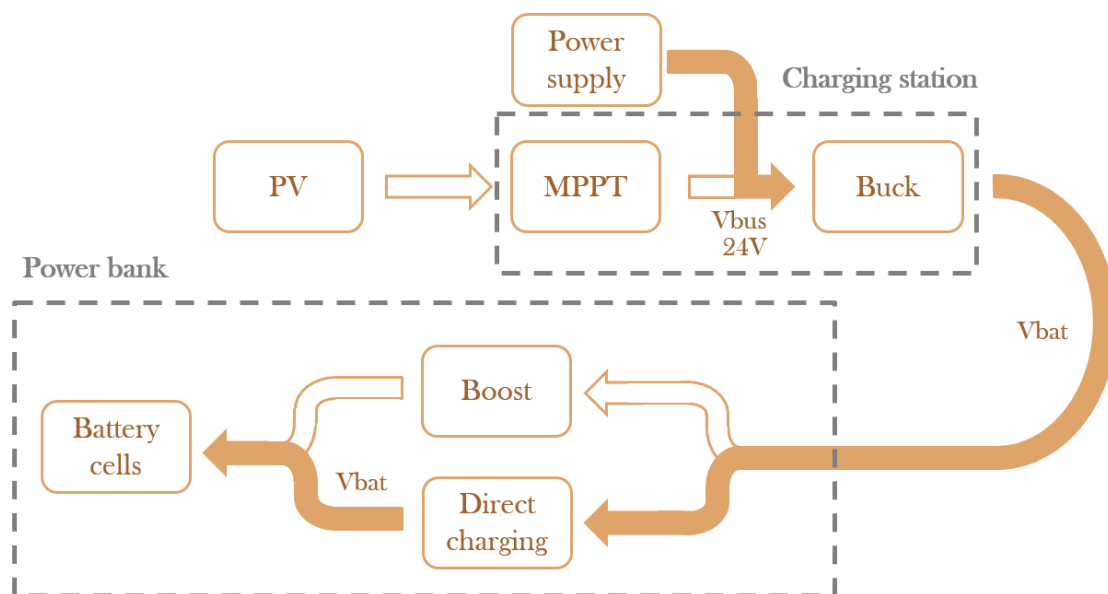
Figure 51: Block-diagram of the battery charging with direct charging

The charging cycle graph in Figure 52 presents a CC/CV charging cycle of the li-ion battery cells. Even though the current reaches values close to 3A at the beginning, the charging current reduces to 1.6A and the charging is performed at constant current during 1h while the voltage of the battery increases gradually. After the 1h mark, the charging changes to constant voltage mode where voltage is more stable and now current varies in a decreasing tendency.

The initial voltage measured in the test is 13.6V which is higher than the under-voltage protection threshold of the BMS. This deviation happens because of the internal resistance of the battery cells , the charging current causes a voltage drop which increases the measured voltage. Before starting the charging, the battery voltage was 12.6V.

The total duration of the charging cycle is 2.5h, although the SoC is not 100% at the end of the test, this is ended when the charging current reaches 10% of the initial value. Another important nuance is that the battery voltage saturates at 15.8V when the charging voltage has been configured at 16.7V. The answer to this inaccuracy is due to the diode on the discharge switch depicted in Figure 45. Power flows through the diode which has a constant voltage drop causing conduction losses.
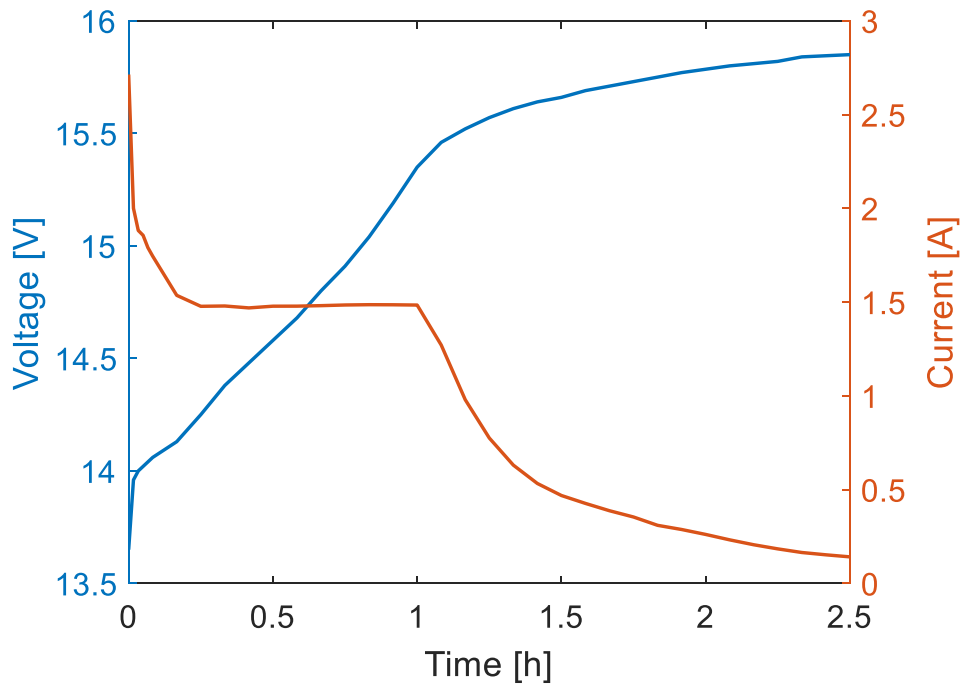
Figure 52: Battery voltage & current results in direct charging test

Another interesting parameter that plays an important role in the relevance of direct charging is the energy consumption. Figure 53 depicts the instantaneous power fed into the cells as well as the cumulative energy to complete the charging cycle. The main outcome of the test is that the battery cells have been charged from depletion to fully charged in 2.5h consuming 37 Wh.
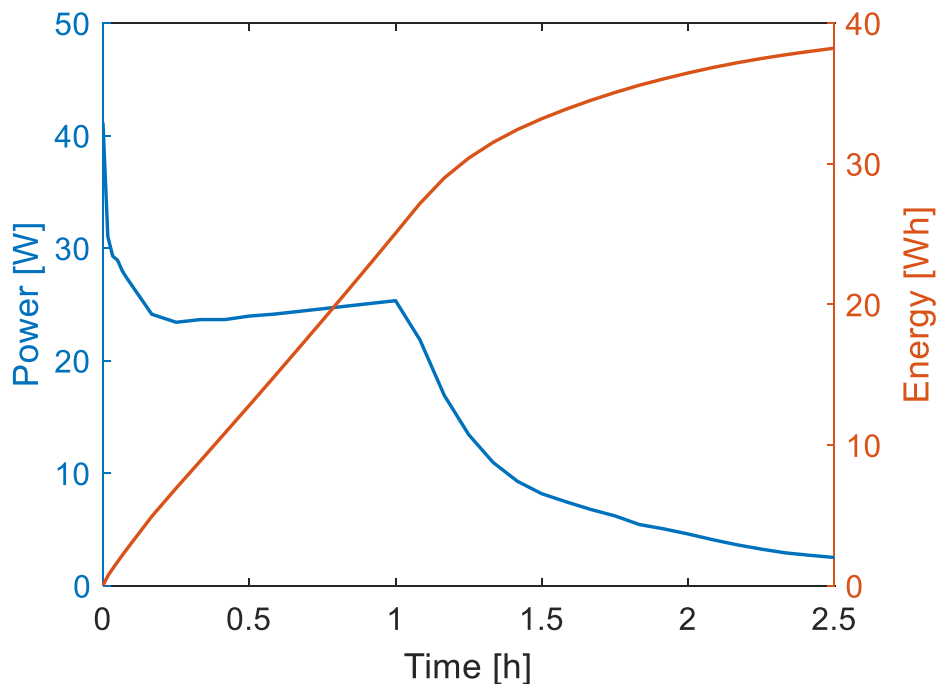
Figure 53: Battery power & energy in direct charging test

6.2 CONVENTIONAL USB CHARGING

The second test intends to simulate the charging process of the battery bank via a standard USB port with 1.5A. The output Buck converter of the solar charging station has been configured according to these parameters. The diagram illustrating the power path of the test is depicted in Figure 54.

A power supply is the source of energy for this test, simulating a PV input. The Buck converter steps-down the 24V bus voltage to an output of 5V and this is taken the power-bank. Given that this voltage is lower than that of the battery cells, the power flows through a Boost converter, which steps-up the voltage to that of the battery cells.
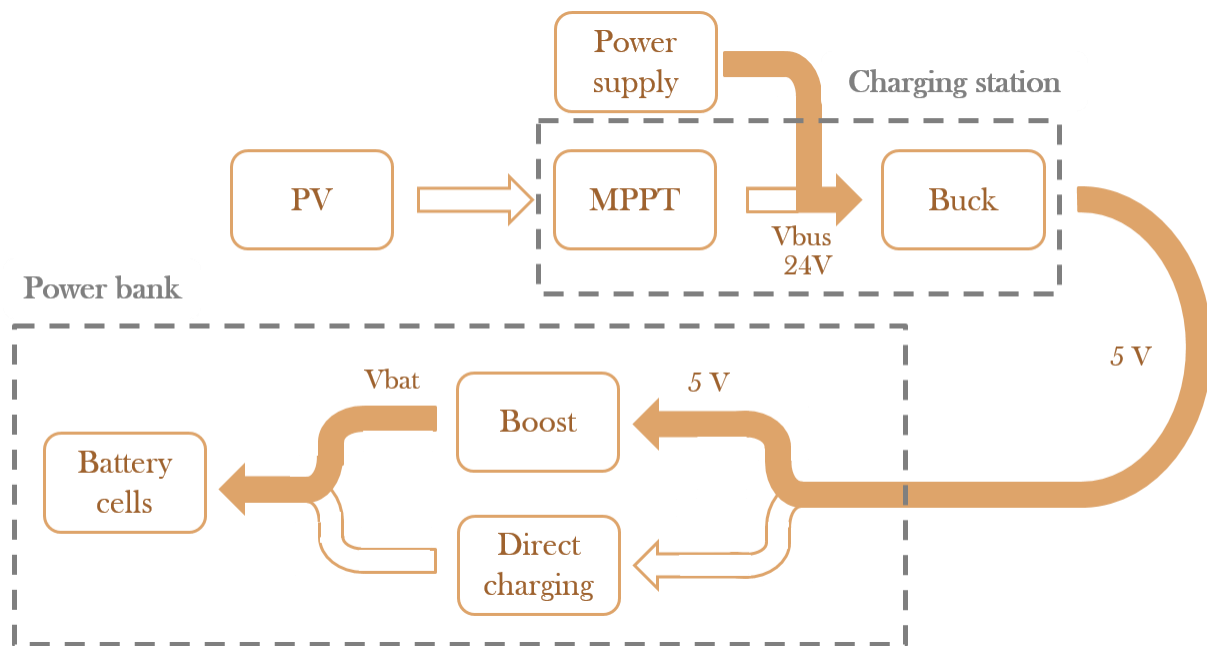
Figure 54: Block-diagram of the battery charging with conventional 5V USB

Various parameters have been measured throughout the test, including battery voltage and current which are illustrated in Figure 55. The figure depicts a timespan of 4h, the reason to show this range is because during this time the total amount of energy taken from the source is the same as for the previous test, 37Wh as shown in Figure 56.

Figure 55 presents a constant current charging cycle, which belongs to the initial stage of a CC/CV charging cycle. The initial value of the battery is 12.71V while charging, before current was flowing the battery had the same voltage as for the previous test, 12.6V. This value increases for 15 minutes and continues increasing for the rest of the test but at a slower pace.

The current of the boost converter input has been limited to 1.5A following the battery charging standard [13]. Converting this to the output of the converter, which is the battery, the current fed into the battery ranges from 0.55A to 0.6A.
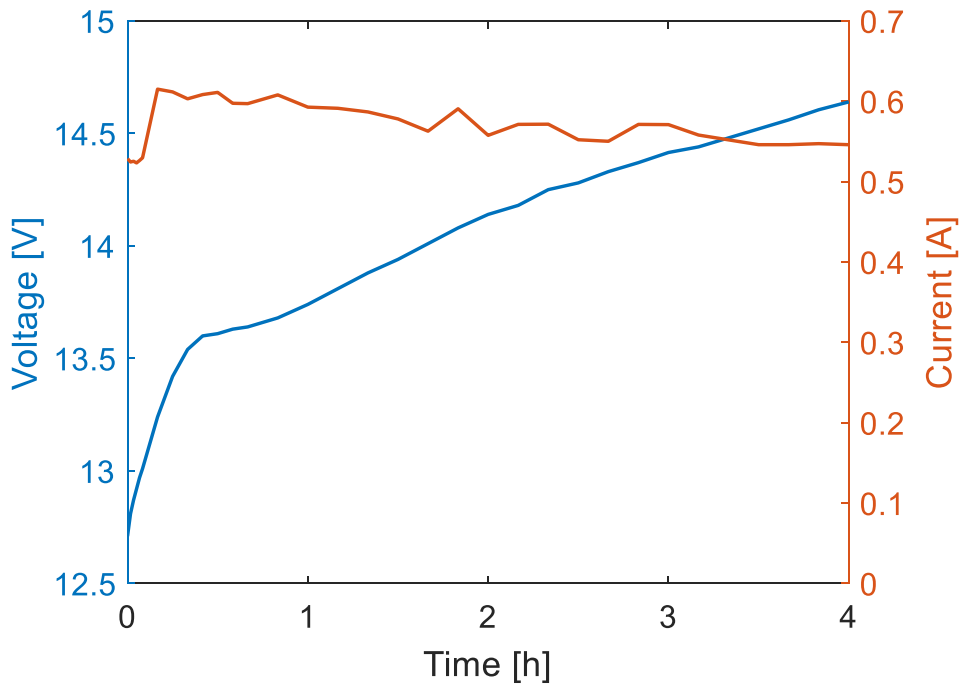
Figure 55: Battery voltage and current results in conventional USB charging test

Figure 56 depicts the instantaneous power fed into the battery cells as well as the cumulative energy. Given that the charging cycle is in constant current mode, the power is relatively constant at 8.5W. The total energy is the same as in the previous test, 37Wh
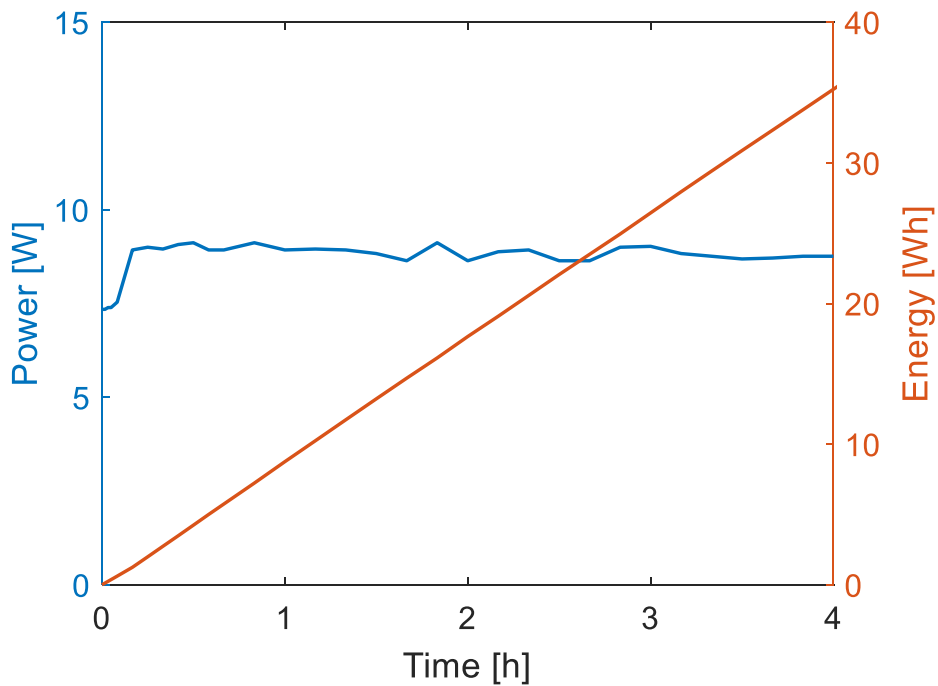
Figure 56: Battery power and energy in conventional USB charging test

6.2.1 SWITCHING PATTERNS OF CONVERTERS

As shown in Figure 54 the power undergoes 2 conversions: a Buck converter at the charging station and a Boost converter at the power bank. These conversions result in switching losses and therefore, lower efficiency. This segment includes the measurements of the switching patterns within the converters.

A) Buck converter

The power coming from the power-supply is first stepped-down from 24V to 5V in an attempt to simulate conventional USB charging. Figure 57 indicates the measurement points of the test:

- The input voltage is represented with green
- The switching node voltage is represented with blue
- The output voltage is represented with red
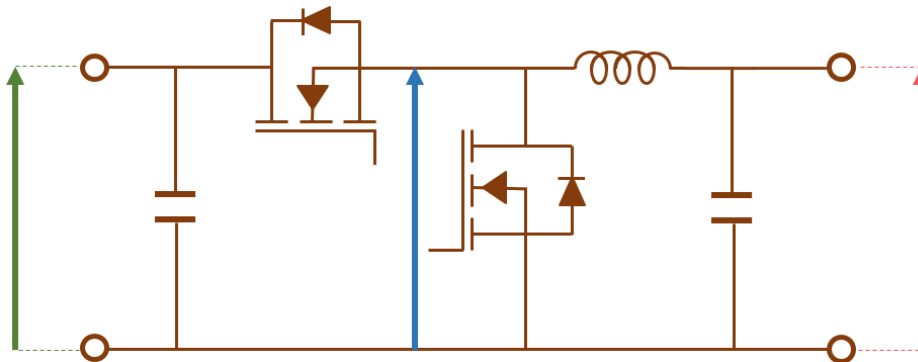
Figure 57: Circuit diagram of a standard Buck converter with measurement points

According to the datasheet of the converter, [20] the frequency is determined with the value of the resistor in one of the pins. For this design a 133kΩ resistor has been placed which is equivalent to 359 kHz. Based on this, the expected period would be 2.786 μs; however, the results in Figure 58 show inconsistent switching pulses. This happens because the converter is in pulse skipping Eco mode. [42]

The TPS5433 is a 3A output Buck converter which regulates the output voltage based on pulse width modulation control. The converter has a minimum ON pulse width that sets the limit of the minimum duty cycle. When the current is low, the converter enters discontinuous conduction mode which is the case of Figure 58 and the IC enters pulse skipping mode in order to minimize losses.

When the low-side switch is on, the blue signal takes the same value as the input voltage. In some cycles, the length of this is longer that it is supposed, a minimum pulse width is established and in order to compensate the following pulses are skipped so that the output voltage is kept at 5V. When the switch is OFF the switching node drops to 0V and halfway through one period, the converter enters DCM.

Even though the switching pattern is in pulse skipping mode, the output voltage is stable at 5V and the input at 24V.
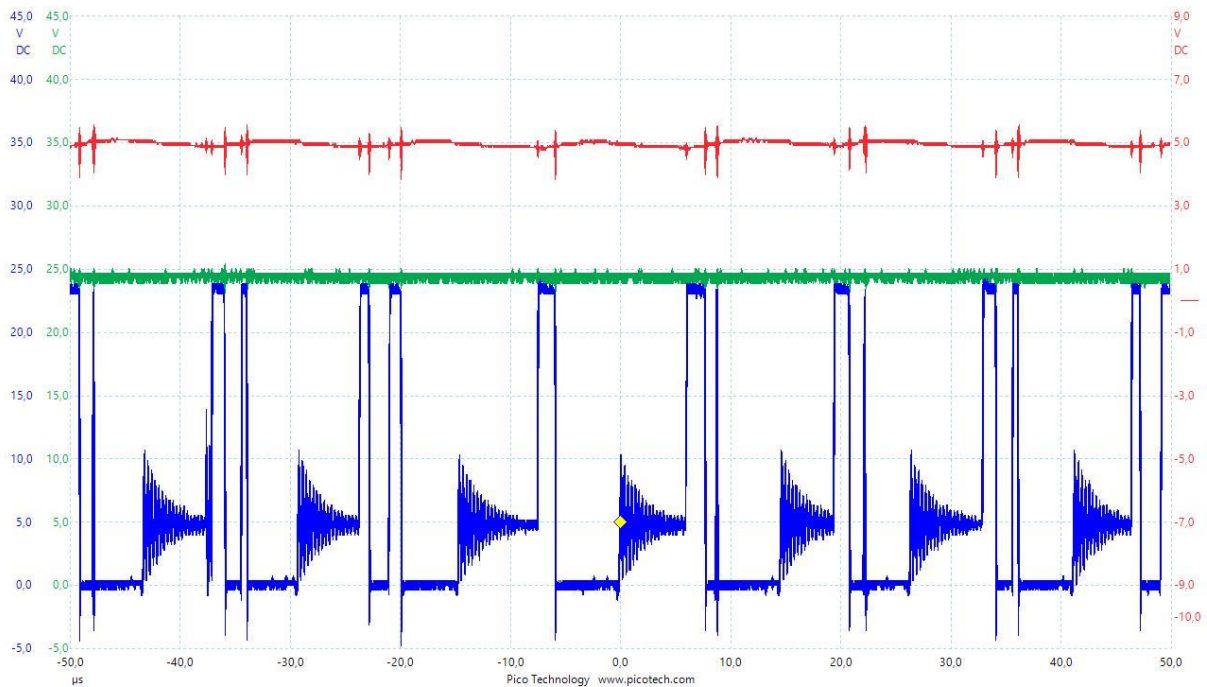
Figure 58: Buck converter switching oscilloscope results

B) *Boost converter*

The second converter is Boost converter that steps-up the 5V from the output of the charging station to the battery cells voltage. Figure 59 depicts the standard configuration of a synchronous boost converter as well as the location of the measurements:

- The input voltage is represented with green
- The switching node voltage is represented with red
- The voltage drop within the inductor is represented with purple
- The output voltage is represented with blue

As it is shown in Figure 60 the timespan between 2 switching instances is 1.839 μs. The switching frequency is adjustable by selecting the value of the resistor in one of the pins of the converter. According to the datasheet of the converter, [43] the frequency would be 500 kHz with a 342 kΩ resistor. In order to stay in that range but utilizing standard resistor values, a 300 kΩ resistor has been placed which leads to a frequency of 544 kHz.
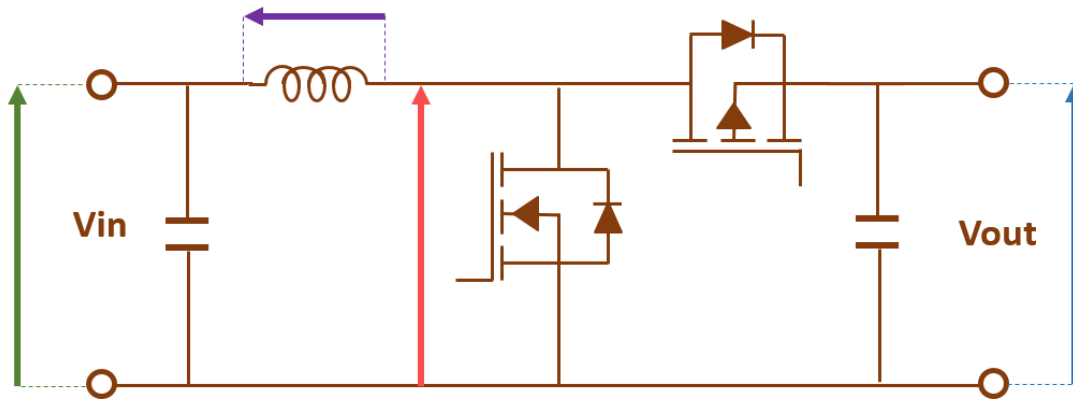
Figure 59: Circuit diagram of a standard Boost converter with measurement points

The input voltage has a relatively stable value of 4.64V with some variation coinciding with the switching of the MOSFETS. The output signal follows the same shape as the input with an average value of 14.49V. While the output of the boost converter is set at 16.7V, the value is determined by the battery cells and is dependent on the SoC. This happens because the converter is in current limiting mode.

The switching node in red presents 2 values in each period: when the low-side switch is OFF, the value is equal to the input voltage. However, when this is switched ON the voltage drops to 0. The voltage drop at the inductor also presents a different behaviour dependant on switching: when the low-side switch is OFF the voltage in *Vin-Vout* which translates to -9.28V and when the FET is ON the voltage is the same as the output voltage. [44]
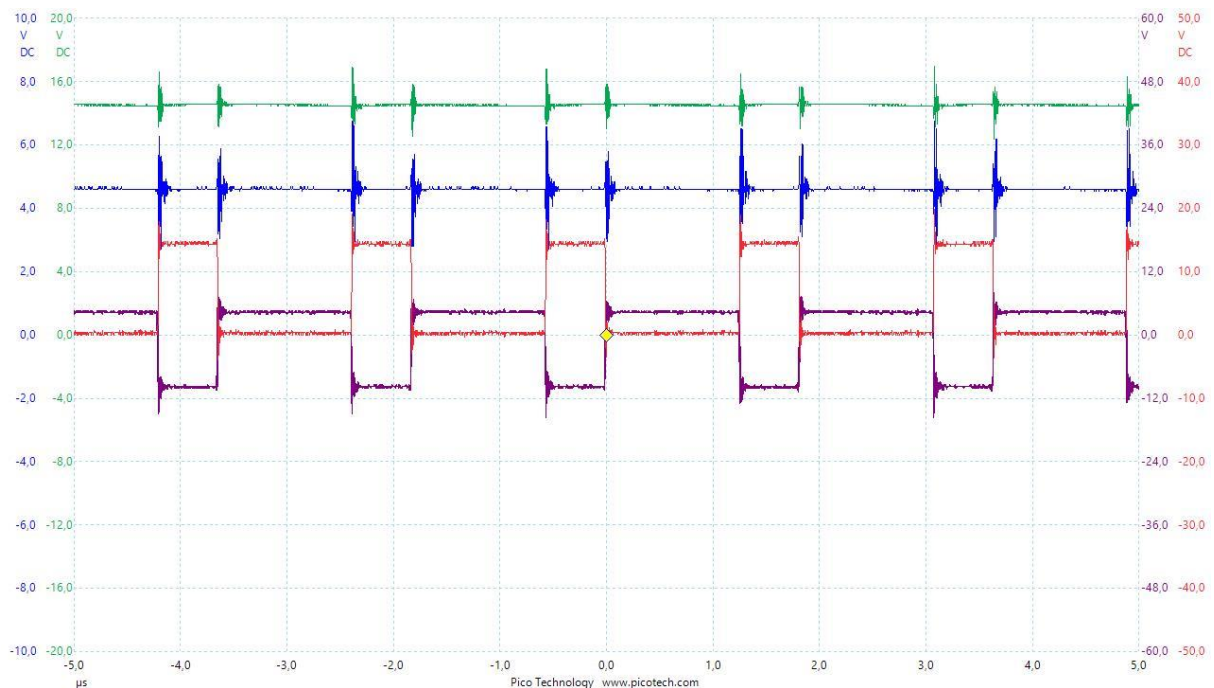
Figure 60: Boost converter switching oscilloscope

6.3 DISCUSSION

The goal of these tests is to make a comparison between the conventional USB charging approach and the direct charging to analyse the performance of each. In order to make an insightful comparison, both test start with the same battery voltage and consume the same input energy.

As far as time is concerned the first test takes 2.5h, which is enough to fully charge the battery from the under-voltage threshold of the BMS to full charge. For the second test, the cycle takes a total of 4 hours in order to consume the same input energy. However, it is important to take into account that as depicted in Figure 53, the power fed into the battery decreases as the charging cycle enters constant voltage mode, hence the battery will charge slower. In order to make a fairer comparison on the time difference it is interesting to pay attention to the energy accumulated within the battery cells in the first hour of the charging cycle. The direct charging accumulates 25 Wh while the conventional USB reaches 8.6 Wh. Based on these numbers, an approximation that can be made is that direct charging is 3 times faster than the conventional USB. The difference between these 2 approaches is due to the following reasons:

- While both tests have been performed at 1.5A at the input of the power-bank, the voltage during the fast charging is, on average, almost 3 times higher than in conventional charging.
- Given that the second approach undergoes 2 conversions, the losses are higher and therefore it will take more time to supply the same energy. Furthermore, when the output voltage of the buck converter is closer to the input bus voltage (24V), the efficiency is higher.
- During the direct charging the current is stabilized at 1.5A, but this could potentially reach 3A increasing the feeding power by 2.
- During the direct charging test, the current flows through the diode at the MOSFET driven by the EN_DSCHRG signal in Figure 45. This diode has a constant voltage drop and generates a significant amount of losses throughout the process. This MOSFET is kept OFF for safety reasons, since it prevents the power to go back and act like a source if the voltage of the supply device decreases. With the correct software configuration, this losses could be avoided.

7. CHAPTER

CONCLUSIONS

The final chapter summarizes the main conclusions that have been drawn throughout the report. A discussion is added reflecting on the research questions posed in Chapter 1. This chapter also intends to shed some light on future lines or improvements that can be applied within the project to increase its potential.

7.1 DISCUSSION OF RESEARCH QUESTIONS

The main outcome of the project is designing and building a working prototype of a SHS to be implemented in a real scenario. During this process, a number of discussions have been present on the research questions of Chapter 1, these are the main conclusions:

7.1.1 HOW TO ADD DYNAMIC ADJUSTMENT OF VOLTAGE AND CURRENT FEATURE TO A STANDARD CONVERTER?

Dynamic adjustment of voltage and limitation of current has been added to the output ports of the solar charging station. This technical task has been discussed throughout Chapter 4. In voltage regulators with variable output, the voltage can be adjusted with a resistor divider from the output to the ground connecting the junction to a reference voltage pin. This task has been tackled by adding elements to this circuit. Adding a third resistor connected to this reference voltage pin with a controlled input voltage will alter the current flows and therefore change the output voltage. For this application, a DAC has been placed to control the voltage signal, this is governed by the MCU through I^2C communication. The chapter also includes a discussion on how the select the values of the resistors that take part in this regulation via Kirchhoff's law; these will determine the output voltage range of the converter.

In order to perform current limitation, 2 operational amplifiers have been added to the output. The first operation amplifier acts as a low-pass filter that measures the current flowing through the shunt resistor placed in the output. A frequency threshold is established to obtain an accurate measurement which is taken to a second operational amplifier that compares the measurement with a controlled signal coming from the DAC. If the measurement voltage is higher that the controllable signal, the diode at the output of the operational amplifier is forward biased and voltage is decreased until current limit is achieved.

The circuit has been implemented on the prototypes and the tests prove that the adjustment successfully follows the circuit design. The design criterion of the components meets important requirements such as: the current measurement after the low-pass filter is accurate. While stability is kept in the control loop and the activation of current limitation is fast enough at 1ms. The outcome is a station with 4 output ports that act like a 60W power supply where voltage can be adjusted and current limited. By developing a circuit with standard market-available products the cost effectiveness criterion is met. Furthermore, the circuit is compatible with a wide range of standard voltage regulators.

7.1.2 HOW TO DESIGN A HIGH-POWER RATE POWER BANK WITH DIRECT/FAST CHARGING?

2 revisions of the power-bank design have been included in Chapter 5. The innovative aspect of the design is the connection in series of the battery cells decreasing current and therefore losses. The converters implemented within the power-bank enable direct charging at the voltage of the battery cells, as well as connecting a wide range of sources operating at different voltages.

The power bank has been tailored for rural electrification applications by implementing functionalities such as the possibility of powering loads while the cells are charging or including 1 high power output port. Nevertheless, the final product is not restricted to developing countries as it counts the characteristics to be utilized in various environments.

7.1.3 WHAT ARE THE BENEFITS OF DIRECT BATTERY CHARGING WITH TYPE C CONNECTION?

The empirical results obtained from the direct battery charging test are addressed in Chapter 6. The content of this segment focuses around the interconnection of the solar charging station as a source with the power-bank. Direct charging has been successfully implemented by feeding power directly to the power-bank from the output of the charging station. 2 tests have been performed with the goal of comparing the performance of direct charging with conventional USB charging at 5V. Various advantages are highlighted within the direct charging process:

- Speed: based on the results of the tests performed in Chapter 6, the average power supplied by the conventional USB charging is 8.2W as opposed to the 23.5W from direct charging during CC charging. This reduces the charging time significantly to approximately 3 times lower. This parameter could potentially be reduced more if direct-charging was performed with 3A instead of 1,5. This feature is especially convenient for rural areas where users cannot charge the power-banks in their homes.
- Efficiency: In the direct charging test, the voltage from the solar charging station bus is stepped down to the battery voltage with a buck converter and then fed directly into the cells with only 1 active converter. For the conventional 5V USB charging, 2 interfaces are present: buck and then boos. Minimizing the number of converters decreases losses and therefore increase efficiency. Furthermore, the efficiency of the buck converter increases as the output voltage increases, hence on this conversion alone, the losses of direct charging will also be lower.
- Cost: being able to charge the power-bank with sources of different voltages requires extra components of energy conversion. The idea of direct charging is a simple circuit that consists of 2 switches in the process of charging. This simplicity reduces the price of the components.

7.2 FUTURE LINES

After building the prototypes and debugging hardware, existing problems within the PCB are identified and as well as potential improvements that result in optimizing prize, operating conditions or reducing volume, for instance. In view of this, and as it has already done with the power-bank, a second revision of the products is necessary. While the direct charging between the solar charging station and power bank was successful proving proper overall operation of the devices, there are some adjustments to be made regarding certain functionalities, for instance the saturation of the charging station output current at 1.5A instead of 3A.

Cost is a limiting factor of the SHS, especially given that its target application is in areas with limited resources. In order to reduce components price in new revisions, the criterion is based on using basic elements such as resistors, capacitors, inductors and switches avoiding dedicated chips that can increase the price. At the moment, the PCBs counts with certain ICs such as the BMS. In future revisions, this task can be performed using basic elements complimented with its software.

Some loads have been connected to the devices and some charging cycles have been performed. However, the products have not been tested at their full capacity, with all 4 output ports of the charging station charging batteries for example. This test is necessary to analyse the losses within the PCB and verify that the temperature stays within normal operating limits. If the thermal test proves losses to be too high, thermal vias and other cooling elements must be included.

The working prototypes will be taken to Ethiopia in some months to perform a pilot test. The purpose of this field test is to obtain feedback from the consumption habits of local villagers and make updates on the products based on this information.

REFERENCES

[1] "World energy outlook," *International Energy Agency,* 2018.

[2] "The World Bank," Sustainable Energy for All, International Energy Agency, Energy Sector Management Assistance Program, 2019. [Online]. Available: https://data.worldbank.org/indicator/eg.elc.accs.ru.zs.

[3] P. Cook, "Infrastructure, rural electrification and development," University of Manchester, UK, 2011.

[4] A. N.Zomers, "Energy for sustainable development," *The challenge of rural electrification,* 2003.

[5] M. T. F. Ognen Stojanovski, "Rural energy access through solar home systems: Use patterns and opportunities for improvement," 2017.

[6] M. Avakian, "National Institute of Environmetal Health Sciences," [Online]. Available: https://www.niehs.nih.gov/research/programs/geh/geh_newsletter/2013/1/spotlight/ kerosene_a_widely_used_fuel_with_unknown_health_risks.cfm.

[7] A. J. Jennifer Tracy, "The true cost of Kerosene in Rural Africa," International Finance Corportaion, 25 April 2012.

[8] T. K. A. Chaurey, "Solar lanterns for domestic lighting in India: Viability of central charging station model," Centre for Energy Studies, Indian Institute of Technology, Hauz Khas, New Delhi, 2009.

[9] N. Wamukonya, "Solar home system electrification as a viable technology option for," *Energy Policy,* 2007.

[10] "New Energy Outlook," Bloomberg new energy finance & PV energy trend, 2018.

[11] "Energypedia," 1 August 2018. [Online]. Available: https://energypedia.info/wiki/Fee-For-Service_or_Pay-As-You-Go_Concepts_for_Photovoltaic_Systems#Basic_Concepts_of_Fee-for-Service_or_Pay-As-You-Go_DESCOs.C2.A0.

[12] G. Manchanda, "Augmenting the diffusion of solar home systems for rural electrification: An Indian perspective," Delft University of Technology, August 2017.

[13] Battery Charging Specification Revision 1.2, 2010.

[14] USB Type & USB Power Delivery - Getting started, "Texas Instruments," 2017. [Online]. Available: http://www.ti.com/interface/usb/type-c-and-power-delivery/getting-started.html.

[15] L. Mackay, N. H. van der Blij, L. Ramírez Elizondo & P. Bauer Toward the universal dc distribution system, Electrical Components and Systems, 2017.

[16] Cree®, "J Series™ 3030 LEDs," Durham, 2017.

[17] R. P. Zero, "Raspberry PI," [Online].
    Available: https://www.raspberrypi.org/products/raspberry-pi-zero/.

[18] M. Integrated, "Digital Adjustment of DC-DC Converter Output Voltage in Portable Applications," August 2016.

[19] T. Instruments, "How to Dynamically Adjust Power Module Output Voltage," December 2016.

[20] T. Instruments, "TPS5433xA 4.5-V to 28-V Input, 3-A Output, Synchronous Step-Down DC-DC Converter," Revised February 2016.

[21] T. Instruments, "QUAD 10-BIT LOW-POWER VOLTAGE OUTPUT I2C INTERFACE DIGITAL TO ANALOG CONVERTER," 2003.

[22] R. Keim, "All About Circuits," 12 May 2019. [Online].

[23] T. Instruments, "INAx181 Bidirectional, low- and high-side voltage output current-sense amplifiers," April 2017.

[24] R. Law, "EEVblog Electronics Community Forum," 2 February 2017. [Online]. Available: https://www.eevblog.com/forum/beginners/adding-cc-to-a-cv-buck-to-make-it-cccv/.

[25] T. Instruments, "TINA-TI SPICE-based analog simulation program," [Online]. Available: http://www.ti.com/tool/TINA-TI.

[26] S. electronics, "Mouser," [Online]. Available:
https://www.mouser.es/new/stmicroelectronics/stm-nucleo-development-boards/.

[27] S.　　　electronics,　　　"STM32　　　IDEs,"　　　[Online].　　　Available:
https://www.st.com/en/development-tools/stm32-ides.html.

[28] Samsung, "Samsung INR1865029E 2900mAh (Blue)," 2015.

[29] K. EDA, 2019. [Online]. Available: http://www.kicad-pcb.org/about/kicad/.

[30] "Electronnic Specifier," 24 February 2010. [Online].
Available:　　　https://www.electronicspecifier.com/micros/stmicroelectronics-locks-in-
stm32-advantages-with-new-megabyte-devices-increasing-application-reach.

[31] ST, 2019. [Online].
Available: https://www.st.com/en/development-tools/stm32cubeide.html.

[32] Battery Management System Tutorial, "Renesas," 2016. [Online]. Available:
https://www.renesas.com/in/en/products/power-management/battery-
management-system-tutorial.html.

[33] T. Instruments, "BQ77915 3-Series to 5-Series Stackable Ultra-Low Power Primary
Protector with Autonomous Cell Balancing and HIBERNATE Mode," March
2018.

[34] S. l. augmented, "Design with surface sensors for touch sensing applications on MCUs,"
2019 Revision 5.

[35] R.S. Components, "Wurth Elektronik," Reverse Mount LED, [Online]. Available:
https://au.rs-online.com/web/p/leds/8154269/.

[36] T. Instruments, "TPS54628 4.5-V to 18-V Input, 6-A Synchronous Step-Down
Converter With Eco-Mode™," December 2016.

[37] NXP, "NX5P3290 USB PD and Type-C current-limited power switch," June 2019.

[38] NXP, "PTN5110 USB PD TCPC PHY IC," 2018 January.

[39] What is the rol of CC pin in Type-C solutions. solution, "Silicon Labs," 26 09 2016.
[Online].　Available:　https://www.silabs.com/community/mcu/8-bit/knowledge-
base.entry.html/2016/09/26/what_s_the_role_ofc-kQYe.

[40] NXP, "NX20P5090 High voltage USB PD power switch," 2016 October.

[41] T. Instruments, "I2C Narrow VDC Buck-Boost Battery Charge Controller With System Power Monitor and Processor Hot Monitor," June 2018.

[42] S. P. a. J. Falin, "Understanding TPS61175's Pulse-Skipping Function," Texas Instruments, July 2009.

[43] T. Instruments, "TPS61178x 20-V, 10-A Fully-Integrated Synchronous Boost with Load Disconnect Control," 2017.

[44] D. W. Hart, Power Electronics, Valparaiso University, Indiana, 2010.

[45] S. B. &. G. P. Jenkins, "Off-grid solar PV: Is it an affordable or appropriate solution for rural electrification in Sub-Saharan African countries?," 2016.